Journal of
Manufacturing and Materials Processing

MDPI

Review

Recent Advances in In Situ 3D Surface Topographical Monitoring for Additive Manufacturing Processes

Vignesh Suresh [1,†], Badrinath Balasubramaniam [2,†], Li-Hsin Yeh [3] and Beiwen Li [4,*]

[1] Alcon Research Laboratories, Fort Worth, TX 76134, USA; vignesh.suresh@alcon.com
[2] School of Electrical and Computer Engineering, University of Georgia, Athens, GA 30605, USA; bb2@uga.edu
[3] Department of Mechanical Engineering, Iowa State University, Ames, IA 50011, USA; lhyeh@iastate.edu
[4] School of Civil, Environmental and Agricultural Engineering, University of Georgia, Athens, GA 30605, USA
* Correspondence: beiwen.li@uga.edu; Tel.: +1-706-542-4011
† These authors contributed equally to this work.

Abstract: Additive manufacturing (AM) has revolutionized production across industries, yet persistent challenges in defect detection and process reliability necessitate advanced in situ monitoring solutions. While non-destructive evaluation (NDE) techniques such as X-ray computed tomography, thermography, and ultrasonic testing have been widely adopted, the critical role of 3D surface topographic monitoring remains underutilized for real-time anomaly detection. This work comprehensively reviews the 3D surface monitoring of AM processes, such as Laser powder bed fusion, directed energy deposition, material extrusion, and material jetting, highlighting the current state and challenges. Furthermore, the article discusses the state-of-the-art advancements in closed-loop feedback control systems, sensor fusion, and machine learning algorithms to integrate 3D surface data with various process signatures to dynamically adjust laser parameters and scan strategies. Guidance has been provided on the best 3D monitoring technique for each of the AM processes. Motivated by manufacturing labor shortages, the high skill required to operate and troubleshoot some of these additive manufacturing techniques, and zero-defect manufacturing goals, this paper also explores the metamorphosis towards autonomous AM systems and adaptive process optimization and explores the role and importance of real-time 3D monitoring in that transition.

Keywords: additive manufacturing; three-dimensional imaging; in situ monitoring; surface topography; process monitoring; defect detection

check for updates

Academic Editor: Steven Y. Liang

Received: 19 March 2025
Revised: 14 April 2025
Accepted: 15 April 2025
Published: 18 April 2025

Citation: Suresh, V.; Balasubramaniam, B.; Yeh, L.-H.; Li, B. Recent Advances in In Situ 3D Surface Topographical Monitoring for Additive Manufacturing Processes. *J. Manuf. Mater. Process.* **2025**, *9*, 133. https://doi.org/10.3390/jmmp9040133

Copyright: © 2025 by the authors. Licensee MDPI, Basel, Switzerland. This article is an open access article distributed under the terms and conditions of the Creative Commons Attribution (CC BY) license (https://creativecommons.org/licenses/by/4.0/).

1. Introduction

Additive manufacturing (AM) is an advanced manufacturing method that constructs a three-dimensional object through a layer-by-layer additive printing of materials. It has enjoyed applications in a variety of industries, including but not limited to transportation [1], fashion [2,3], health [4], and food [5]. Despite rapid growth in this field, challenges still exist in AM technologies, such as porosities, anisotropic properties, and non-uniformity generated during the printing process. These challenges have motivated researchers to investigate non-destructive evaluation (NDE) techniques such that these process defects can be actually identified, positioned, labeled, and potentially rectified within or after the process.

In the field of AM, the implementation of NDE techniques is flourishing, driven by the need to address some well-known fundamental issues (e.g., porosities, anisotropic properties, and non-uniformity) in the process. Leak testing, or the liquid penetration

test [6], is a straightforward approach to identify discontinuities in printed solid material. However, such an approach can only be used after the manufacturing process and thus is not suitable for in situ NDE. Microwave NDE [7] can be a great approach to characterize the printing process using plastic or organic materials, yet such an approach is difficult to implement in metal AM due to the limited penetration capability of microwaves. Eddy current testing [8] has been proven effective in characterizing electrically conductive materials or materials with magnetic permeability. However, it is difficult for such technology to precisely locate and quantify the size of defects. Ultrasonic testing [9] can be a great tool to identify defects in structures printed with any solid material that affects sound attenuation, yet the inspection of small or irregular-shaped defects may be difficult for such technology. Computed tomography (CT) [10] and micro-CT [11] have been extensively used in the AM industry due to their capability of visualizing the internal structures of any solid materials through sliced layer-wise imaging. However, the time taken to complete the whole imaging process (e.g., in hours) makes it prohibitive to implement it for in situ monitoring. Thermographic imaging [12] is by far the most widely studied in situ NDE method for AM, given its capability of high-speed temperature field monitoring and prediction of defect existence, although precisely predicting or identifying the size of defects might still be a challenging task.

Even though many different sensing modalities have been well established in the NDE of AM, the importance of another unique modality, surface topography, has not been well-studied at the current stage. Various parameters, such as surface finish [13] and the signature of the manufacturing process [14], can be evaluated using the surface topography. The surface topography is also useful in optimizing the AM process. Additionally, 3D monitoring can provide valuable geometric data regarding layer adhesion and structural integrity in the case of the extrusion process, droplet shape and formation in the case of the jetting process, and melt pool parameters in the case of the energy deposition and powder bed fusion processes. These data can be used in conjunction with machine learning algorithms for autonomous, fine-grained process control to tend towards a fully automated, zero-defect process, something that has been a long-standing goal of additive manufacturing. To this end, there is a need for a comprehensive review of 3D monitoring techniques in additive manufacturing processes. Our article introduces various additive manufacturing techniques, discusses the state of 3D monitoring in each of them by performing a comprehensive literature review, and also examines the state of closed-loop feedback control, highlighting the significance of 3D monitoring in these processes.

This paper is organized as follows: Section 2 will discuss our distinction from existing review articles, Section 3 will introduce the principle of various AM processes, Section 4 will discuss the principle of the various 3D topography monitoring methods, Section 5 will summarize the various research articles on in situ 3D topography monitoring for AM processes, Section 6 will discuss the prospects for future work, and Section 7 summarizes the paper.

2. Distinctions from Existing Review Articles

We have summarized review articles relevant to this topic in Table 1.

It is clear from Table 1 that most of the related review articles on this topic either focus on one type of additive manufacturing method or do not expound upon in situ 3D monitoring techniques in enough detail.

Given the increasing demand for using advanced 3D methods such as laser scanners, structured light scanning, and optical coherence tomography to improve the AM process and their usefulness in each, it is necessary to provide a review of the various state-of-the-art research works that have developed 3D monitoring methods for AM processes. It is

also necessary to provide a comprehensive review of their impact on each kind of additive manufacturing process.

Table 1. Summary of reviewed papers on additive manufacturing monitoring techniques.

Article	AM Process	Sensing Modality	Primary Use of 3D Monitoring
Cai et al. [15]	Metal-based laser additive manufacturing	Optical, thermal, and acoustic	Low: more focused on AI-assisted 2D monitoring instead
Ozel [16]	Fusion-based methods	Optical, thermal, and acoustic	Low: the author explores all sensing modalities and does not explicitly focus on 3D monitoring
Aydogan and Chou [17]	Laser bed powder fusion	Optical, thermal, acoustic, and X-ray	Low: the authors focus on multiple sensing modalities and not explicitly on 3D monitoring
Balhara et al. [18]	Fusion-based metal additive processes	Imaging techniques	Low: the authors focus more on 2D imaging techniques and discuss the strengths of high-speed imaging, thermal camera, and digital cameras
Chen et al. [19]	Fusion-based metal additive processes	Imaging techniques	Low: the authors primarily focused on 2D, high-speed imaging in combination with AI
AbouelNour and Gupta [20]	Powder bed fusion and fused filament fabrication	Optical, thermal, acoustic, and X-ray	Moderate: the authors mention both 2D and 3D monitoring methods; however, they limit their context to internal defect detection in these processes
Zhang et al. [21]	Metal additive manufacturing	Imaging techniques	Low: the focus is on 2D imaging rather than 3D monitoring
Xia et al. [22]	Wire arc manufacturing system	Imaging techniques	Moderate: the authors perform a review of all sensing modalities, including vision, thermal, spectral, and acoustic-based sensing, with 3D monitoring not being their sole focus
Lu and Wong [23]	Examines challenges to implement thermal and acoustic NDT for AM processes, not process-specific	Thermography and acoustic techniques	None: focuses on thermography and acoustic methods
Everton et al. [24]	Powder bed fusion and direct energy deposition	Thermal, acoustic, and optical methods	Low: primarily focus on 2D monitoring
Oleff et al. [25]	Metal extrusion additive manufacturing	Thermal, acoustic, and optical methods	Moderate: the authors cite review articles that used structured light, stereo vision, and laser triangulation for material extrusion; however, 3D monitoring was not their sole focus
Jacob et al. [26]	Fused filament fabrication (material extrusion process)	Imaging techniques	None: the authors reviewed the different metals used in the fabrication process and discussed the limitations in the process but did not perform a review on 3D monitoring techniques used for extrusion process
Vora et al. [27]	All AM processes	Multiple sensing modalities are mentioned including acoustic, thermal, and optical techniques	None: the authors briefly describe the merits and demerits of each sensing modality, including 3D monitoring, but do not perform a review of literature in this area

In this paper, we have reviewed various in situ 3D topography monitoring methods for AM processes. We have classified the various research works into four categories: in situ 3D monitoring methods for (i) powder bed fusion, (ii) direct energy deposition, (iii) material extrusion, and (iv) material jetting. The scope of this paper encompasses several critical aspects of AM monitoring and control. Firstly, it provides a concise introduction to each AM method, elucidating the underlying principles and addressing the potential challenges associated with in situ monitoring for each technique. Secondly, the paper expounds upon diverse 3D topography monitoring techniques, explaining their mechanisms and discussing the challenges of implementation within AM processes. Thirdly, it presents a comprehensive survey of existing literature on in situ 3D monitoring for each of these AM techniques, analyzing their respective advantages and limitations. Furthermore, this review article delves into the current state of closed-loop feedback control in AM processes, exploring the path towards full automation and the role of 3D monitoring in this endeavor. This aspect is particularly significant in the context of Industry 4.0 and the integration of artificial intelligence in manufacturing processes. To the best of our knowledge, this review article represents a novel contribution to the field, as it uniquely explores in situ 3D monitoring within the context of additive manufacturing, offering a comprehensive literature survey on 3D monitoring techniques in AM. By examining the current state of closed-loop feedback control in AM, its future prospects, and the instrumental role of 3D monitoring in achieving fully autonomous processes, this paper provides valuable insights into cutting-edge developments in this rapidly evolving domain.

3. Working Principle of Additive Manufacturing Processes

3.1. Powder Bed Fusion

Powder bed fusion (PBF) is one of the most well-developed AM technologies [28,29]. PBF was invented in the 1990s. The method involves spraying powder material on the powder bed surface and fusing it with a thermal energy source (as shown in Figure 1). This process is repeated for each layer of printing. Based on the type of thermal energy, there are two types of powder bed fusion process: (i) laser sintering (which uses a laser source) and (ii) electron beam melting (uses electron beam). This method is used for printing ceramics, metals (such as aluminium, titanium, and cobalt) and plastic materials. Laser power, layer thickness, laser scan velocity, and hatch distance are some of the important process parameters. It does not require any support structure, and complex geometries can be fabricated. Except for the electron beam melting process (which requires vacuum conditions), PBF methods do not require any specific operating conditions. However, a major limitation is that the built object has high porosity when the powder cannot be fused completely [30].

Conventional online monitoring of PBF processes, especially the monitoring technology based on optical imaging, is subject to many challenges, namely lighting, metal evaporation, and temperature [31]. Additionally, sensing methods used in research studies are expensive or difficult to install in industrial machines.

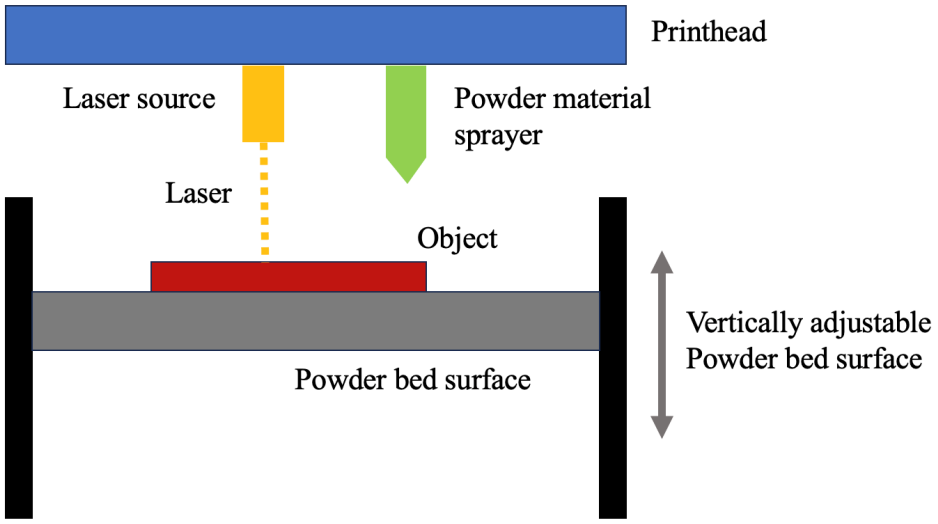


Figure 1. Powerbed fusion schematic diagram.

3.2. Direct Energy Deposition

Direct energy deposition (DED) was first developed in the 1990s. DED involves fusing a metal powder/wire using a direct energy source such as a laser [32,33]. A schematic of the DED process is illustrated in Figure 2. The melted metal wire is deposited on the building surface. Most DED processes require a sealed chamber, vacuum, or inert gas operating conditions. Laser power, spot size, and feed rate are some of the important process parameters. This method can be used only for manufacturing metals. This method is widely used for the repair of parts in re-manufacturing processes. However, the accuracy of this method may be limited [34].

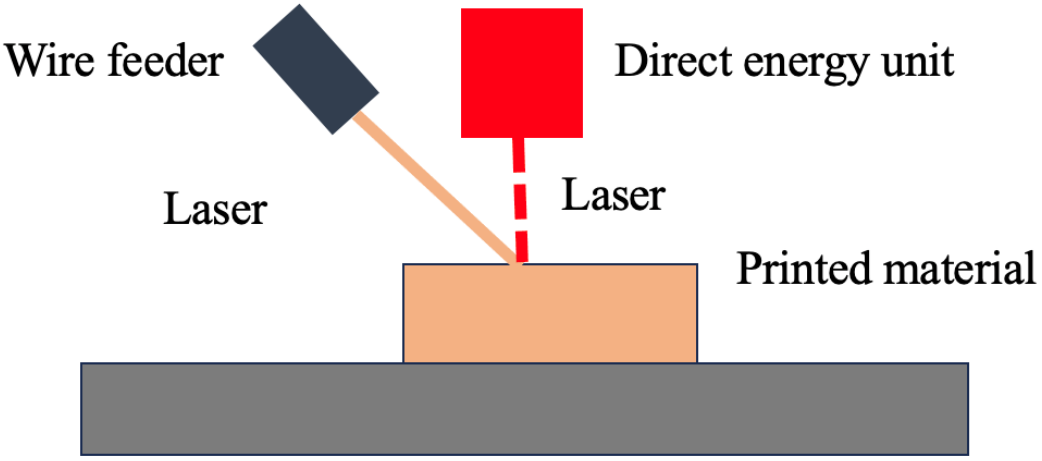


Figure 2. Direct energy deposition schematic diagram.

In the DED process, process signatures such as the temperature, width, length, and height of the melt pool are directly correlated with the quality of the final product and can be used to detect potential defects. The complex process environment makes it difficult to monitor process signatures. Heat source interference, spatter interference, small size, dynamic nature, and intense brightness of the molten pool make it difficult to acquire images in the visible spectrum. Images in the infrared (IR) spectrum are acquired to monitor the temperature distribution of the melt pool, a vital process signature in DED. However, care must be taken to ensure that an optical filter that eliminates the wavelength

range of a laser beam is used because the wavelength range of some laser sources and IR cameras overlap [35].

3.3. Material Extrusion

Material extrusion is one of the most economical AM methods. This method was invented in the 1980s. It is otherwise referred to as fused deposition modeling (FDM)/fused filament fabrication (FFF). In this method, the printing material (such as filament and clay) is extruded through a print head (as shown in Figure 3). The print head is heated to melt the filaments before deposition [36]. This process repeats, and the filament is extruded layer by layer. The method can be used for fabricating polymers and plastics. Layer height, extrusion rate, print speed, and nozzle diameter are some of the important process parameters. It does not require any special operating conditions. As the nature of the build process hinges on a direct extrusion of material, the printing speed is limited [37]. Developing a cost-effective and efficient monitoring setup is a major challenge that requires a deep understanding of the AM process and instrumentation. An active research thrust in in situ monitoring for this process involves the use of sensor fusion for data acquisition and machine learning (ML) models to obtain complex information such as the events that lead to defect formation, defect characterization by type, proactive product failure location estimation, and even optimize process parameters [20].

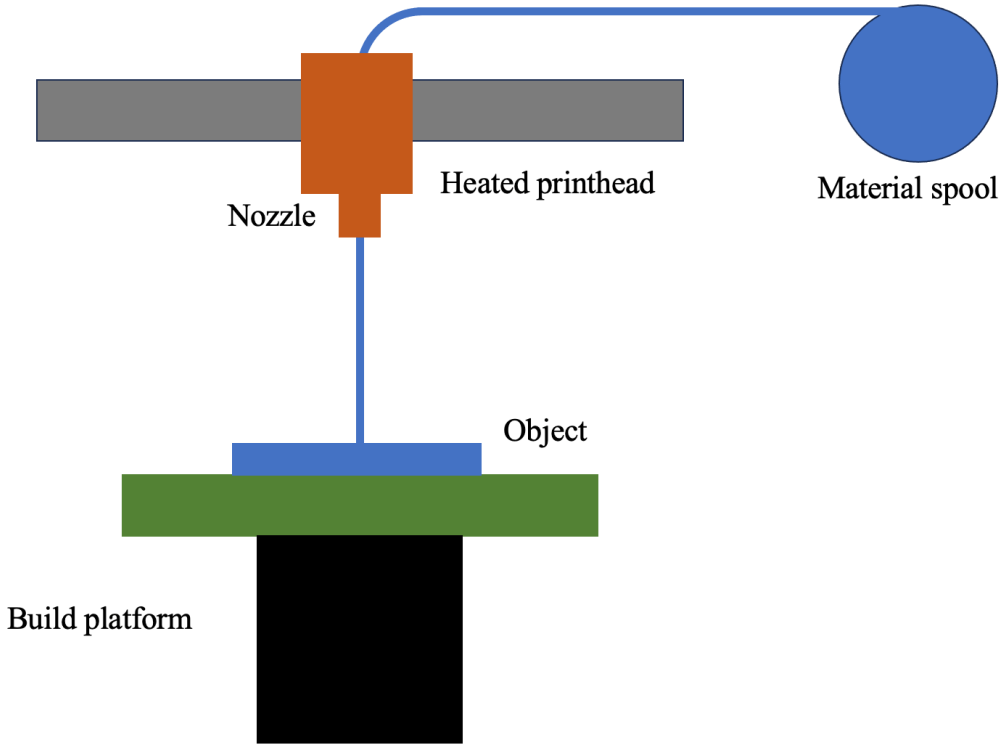


Figure 3. Material extrusion schematic diagram.

3.4. Material Jetting

Material jetting was invented in the 1990s. The method involves the deposition of the print material on the build platform using a thermal or a piezoelectric method. The material is deposited in the form of droplets and is cured by ultraviolet light [38,39]. The method requires a support structure during the build process (as shown in Figure 4). This method can be used for the fabrication of polymers and plastics. Printing orientation, nozzle cleanliness, and layer thickness are some of the important process parameters. Because the

material is deposited in drops, this method has low waste. However, the type of material that can be printed is limited (such as polymers and waxes).

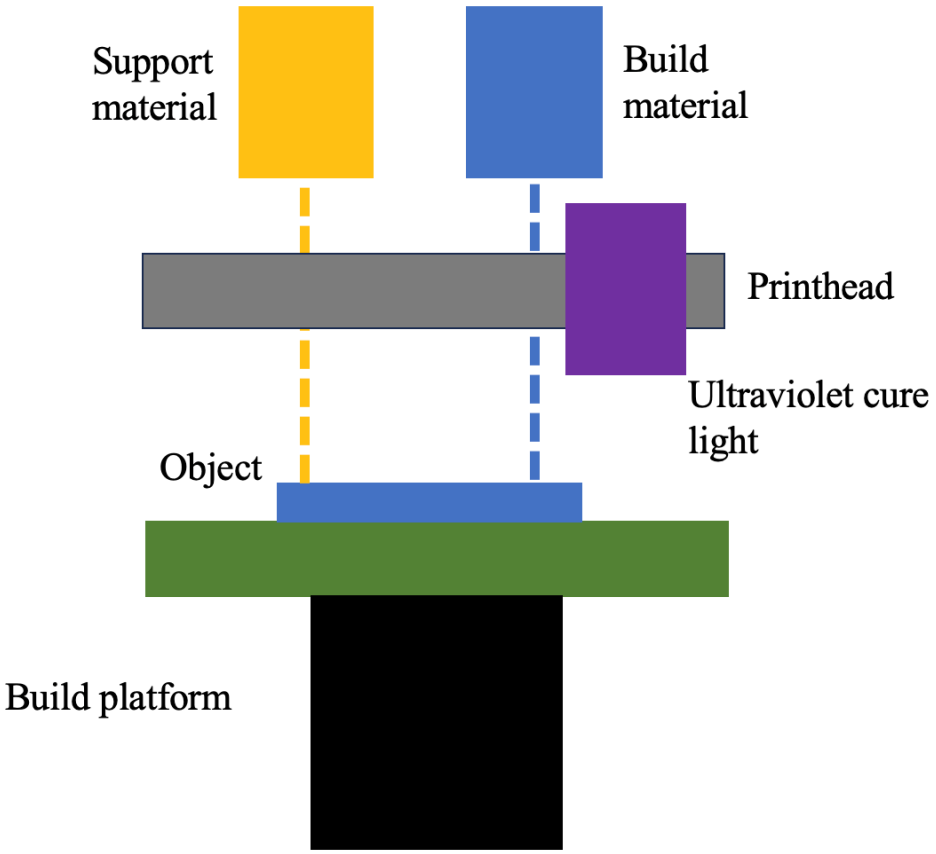


Figure 4. Material jetting schematic diagram.

Variations in input process parameters and fluid properties can significantly impact print quality, making consistent monitoring difficult. These variations affect critical droplet attributes, including droplet size, velocity, aspect ratio, and presence of satellite droplets [40]. Furthermore, closed process chambers for certain material jetting operations can make installation of monitoring equipment difficult [41].

3.5. Vat Photopolymerization

Vat photopolymerization was invented in the 1970s. The method involves the deposition of the resin material on the building platform [42]. The resin is solidified using ultraviolet light. The entire setup is placed in a pool of vat (as illustrated in Figure 5). Based on the type of light source or polymerization mechanism (for solidification), there are different types of vat photopolymerization, such as stereolithography, digital light processing, and liquid crystal display. The vat is drained after completing the build process. This method is used for building objects with complicated structures. Like material jetting, this method can also be used for the fabrication of polymers and plastics. Build orientation, layer thickness, and strain rate are some of the important process parameters. However, the build size and strength of the part are limited [43].

In order to continuously image the process and monitor the material, any camera setup needs to be able to view the resin through the vat. Additionally, imaging the dynamic melt pool generated when the resin is cured by the laser is a challenging task due to saturation and the dynamic nature of the process [44].

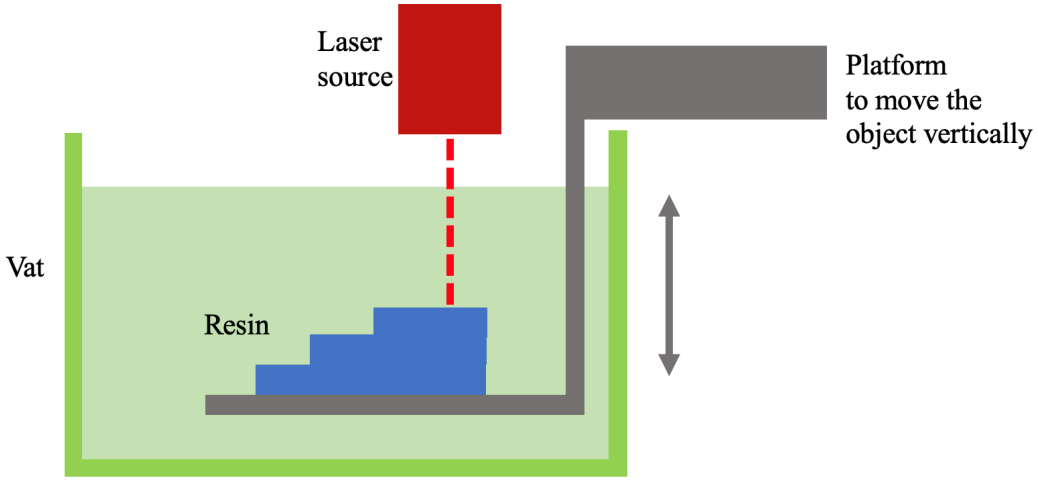


Figure 5. VAT photopolymerization schematic diagram.

3.6. Binder Jetting

Binder jetting was developed in the early 1990s. The process involves spreading the powder material on the build surface using a roller and binding the powder using an adhesive [45]. The build platform is lowered after the deposition of the adhesive to build the next layer (as shown in Figure 6). Binder jetting can be used to fabricate polymers, ceramics, and metals. Layer height, print head speed, and number of nozzles are some of the important process parameters. Binder jetting is an efficient and affordable technique, and a smooth surface finish can be achieved with low roughness [46]. However, the structural strength of the parts is limited as the strength depends on the binding of the powders [47].

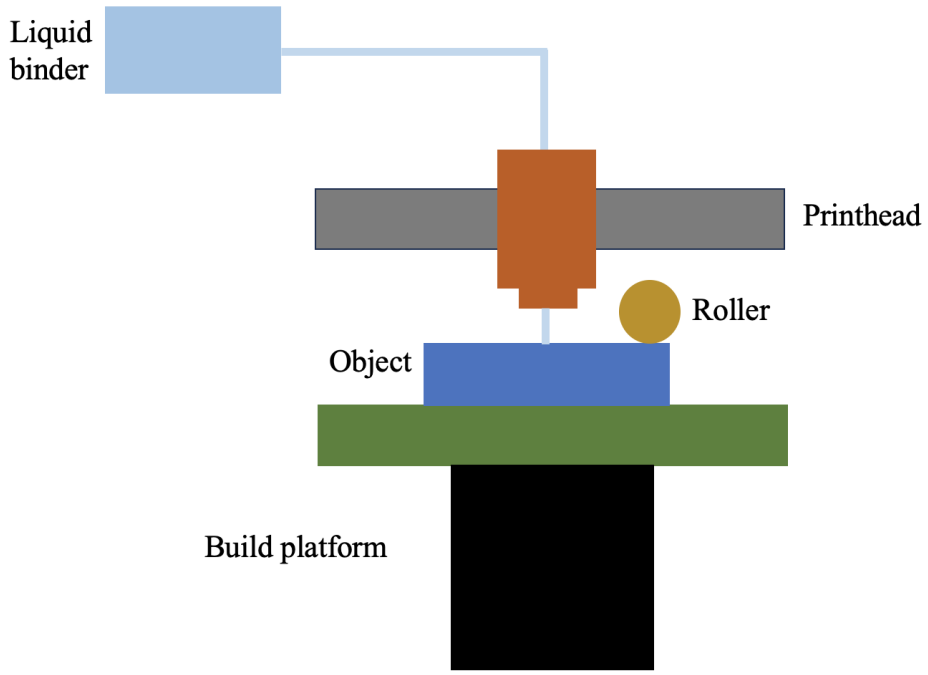


Figure 6. Binder jetting schematic diagram.

Parameters like binder droplet shape, droplet impact points, droplet velocity, and impact ratio influence the quality of the final product, but due to their high speed, small size, and dynamic nature, it is difficult to monitor continuously. Similarly, powder bed interactions are also important to be monitored. Droplet impact causes powder particle

movement and ejection, and ejected particles can form depletion zones that lead to dimensional inaccuracies. Therefore, it is important to monitor and effectively capture this phenomenon using 3D monitoring, but their small sizes and the dynamic nature of the process make them difficult to capture. Additionally, a closed process chamber can restrict access to monitoring equipment.

Parab et al. [48] conducted high-speed in situ monitoring of this process using X-ray imaging. They attempted to study the dynamics of generation and deposition of binder droplets to ensure reliability in the geometry and quality of printed parts. They also leveraged the capability of X-rays to observe sub-surface behavior to study interaction depth and powder ejection, which can also contribute towards the quality of the final part.

3.7. Sheet Lamination

The sheet lamination method was invented in the 1990s. It involves binding thin sheets of material either by ultrasonic welding (ultrasonic additive manufacturing) or by adhesives (laminated object manufacturing). The desired shape is etched by striking the laser on the sheets [49]. The metal sheets are supplied onto the build surface using a roller (as shown in Figure 7) for each layer of printing. Any material that can be rolled (such as paper, sheets, and polymers) can be fabricated by this method. Roller temperature, roller speed, and laser cutting time are some of the important process parameters. The main advantage of this method is that it does not require any support structures. However, the method is time-consuming and produces more waste compared to other AM methods [50].

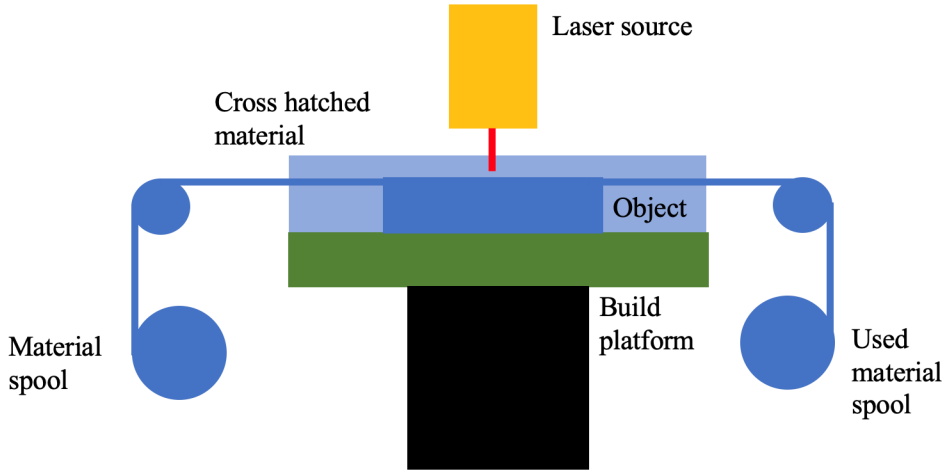


Figure 7. Sheet lamination schematic diagram.

The layering of sheets and the subsequent bonding process can obstruct the continuous monitoring of the entire build volume. Enclosed build chambers, often required for temperature control, can restrict access to monitoring equipment. High-intensity radiation or inadequate lighting conditions may interfere with optical monitoring systems.

4. Three-Dimensional Topography Monitoring Technologies

4.1. Digital Image Correlation

Digital image correlation (DIC) is one of the simplest non-contact optical methods that is primarily used for estimating the 2D displacement of an object. Recently, researchers have developed 3D displacement estimation methods using DIC [51–53]. A typical DIC system only requires a camera, an illumination source, and speckle patterns on the surface of the object. The speckle patterns can be generated using simulations [54]. The speckle patterns are projected on the surface of the object, and the camera captures images of the object (with the speckles) before and after displacement. The DIC method divides the image into

small windows, and this window region is searched in the other image. Once the matching window is identified, the displacement is estimated using the difference in the position of the window centers in the two images. For 3D measurements, the system will include two cameras. A triangulation will be established between the two camera images and the object surface. The correspondence between the camera images is established using the speckle patterns. The system setup of DIC is simple as it only requires cameras to estimate the 3D shape or displacement. However, the method is not robust as the accuracy of the DIC relies on the ability to have unique patterns (speckles) on the object's surface to perform measurements. Figure 8 shows a digital image correlation setup for wire and arc additive manufacturing. These speckle patterns must be clearly visible on the object's surface before any measurement is made. Metallic surfaces and melt pools, which are common in AM processes like powder bed fusion, pose problems of saturation, and overexposure, and this can make it challenging to monitor them using DIC. Similarly, complex structures that are frequently made using AM processes, such as material extrusion, can cause occlusion and shadow issues, which can make the occluded issues challenging to measure using this technique.

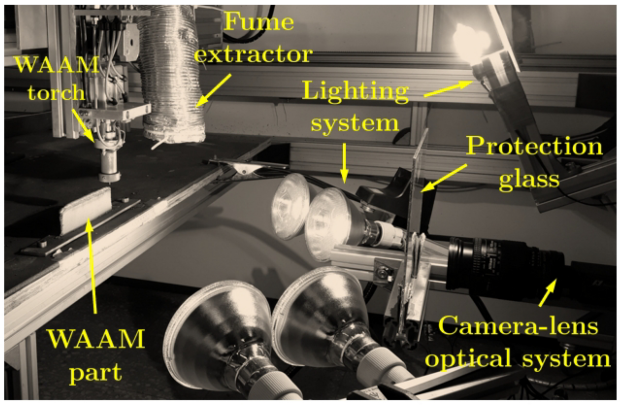


Figure 8. Schematic of the digital image correlation setup for wire and arc additive manufacturing processes (reused from [41]).

4.2. Laser Scanning

Laser scanning is one of the well-established non-contact 3D shape measurement methods. The setup consists of a laser source (emitter) and a camera [55–57]. The laser source projects a line of laser light on the object. On striking the surface of the object, the laser light is reflected and recorded by a detector (camera). The depth information is estimated by triangulating among the laser source, the reflection point on the surface, and the point recorded on the camera. The schematic of a typical laser scanner is illustrated in Figure 9. Laser scanners are well commercialized, and many products are available on the market (such as Zeiss, Keyence, and FARO 3D scanners). Manufacturing industries use laser scanners for quality inspection purposes. Figure 10 shows a setup of a laser scanner used in the in situ monitoring of the powder bed fusion process. The main advantage of laser scanners is that they are easy to operate. However, laser scanners are limited in accuracy, and it is time-consuming to scan large objects as the scanner has to be moved across the entire surface of the object. They can still be used for layer-by-layer process monitoring, but their slow speed makes them impractical for real-time AM process monitoring and closed-loop feedback control.

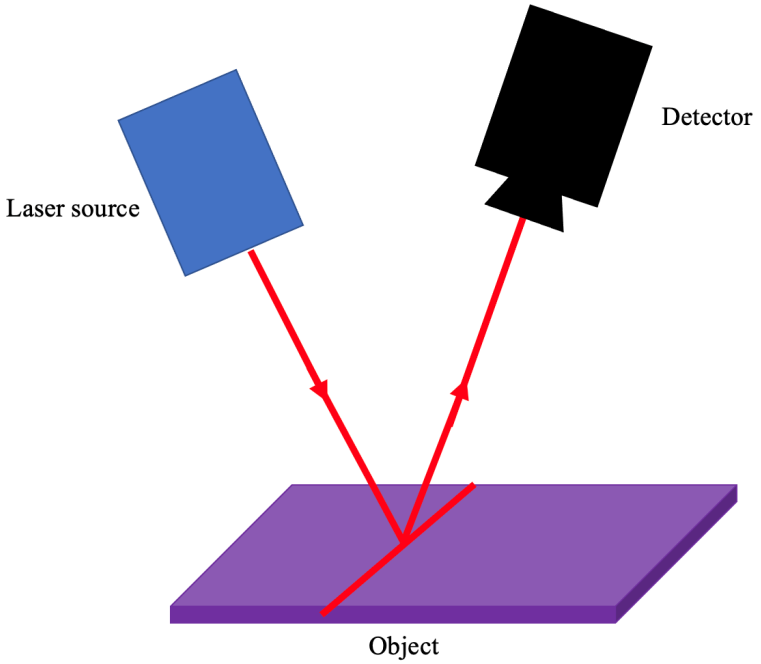


Figure 9. Schematic of the laser scanner.

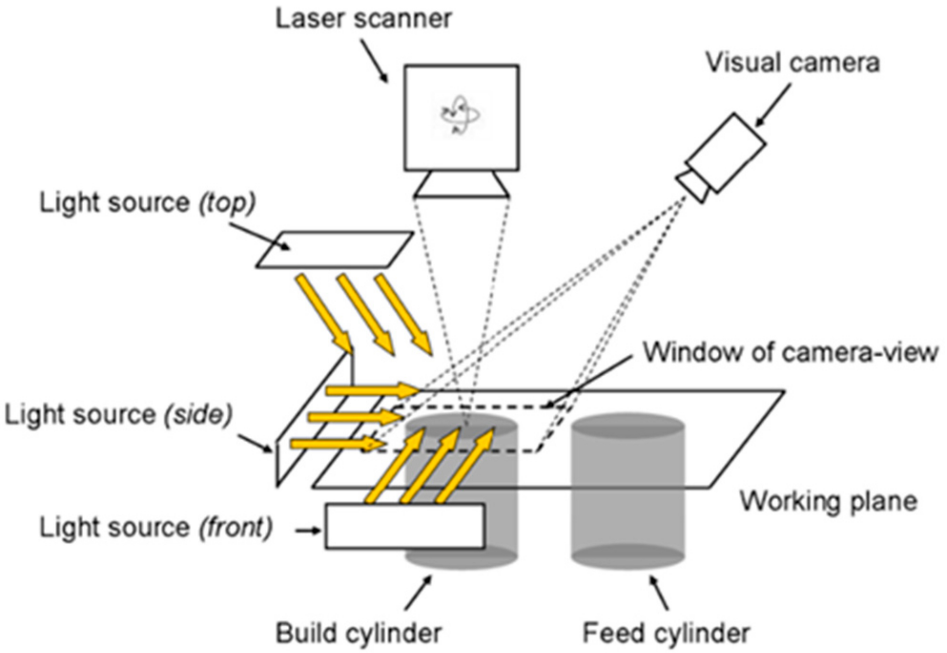


Figure 10. Laser scanner used in the in situ monitoring of the powder bed fusion process (reused from [31]).

4.3. Structured Light

The structured light method is the next-generation stereoscopic system that uses a projector and camera to estimate the depth information of the objects being captured. Unlike the stereoscopic system, this method does not have the limitation of finding correspondence between the camera images of objects with a uniform texture. This is because the system has an active illumination device (projector) that projects codified fringe patterns for establishing correspondence. Structured light systems can have different types of codifications, such as random [58], binary [59], N-ary [60], and sinusoidal patterns [61]. A structured light system with sinusoidal patterns is called a digital fringe projection (DFP) system. In DFP

systems, there are two approaches to analyzing fringe patterns: (i) the Fourier transform and (ii) phase-shifting profilometry. The phase-shifting technique is by far the most accurate method for fringe analysis. The schematic of a typical structured light system is illustrated in Figure 11. The two main components of the system are a projector (A) and a camera (B). The projector, camera, and object (C) form a triangulation base. The triangulation relationship is established by calibrating the projector and camera [62,63]. The projector projects codified fringe patterns on the object. The fringes are distorted based on the object's topography, which is captured by the camera. These distorted fringe images are analyzed using phase-shifting algorithms. Typically, a series of fringe images with equal phase shifts are projected onto the object. The phase map for estimating the 3D coordinates of the object is obtained from these fringe images. If more fringe images are used, the average noise in the phase map will be reduced. The 3D coordinates can be obtained from the phase map. Figure 12 shows a four-camera fringe projection system installed inside a mock powder bed fusion chamber.

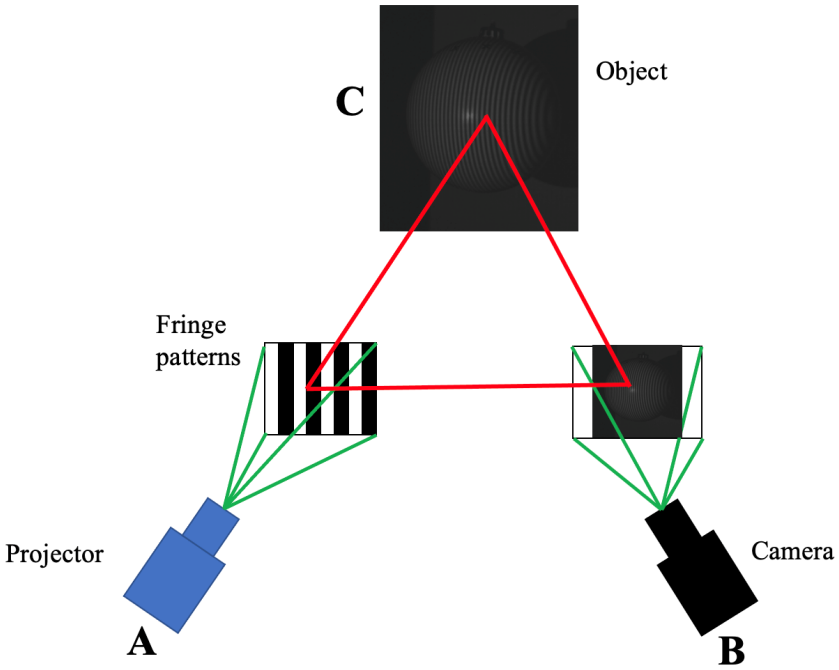


Figure 11. Schematicof the structured light system consisting of Projector (A), Camera (B) and Object to be scanned (C).

Structured light systems suffer from two types of artifacts: (i) saturation-induced errors and (ii) motion-induced errors. Saturation-induced errors typically occur while imaging objects with highly reflective surfaces, as the fringe patterns are masked by the saturation caused by projector illumination [64]. This challenge is especially pertinent to additive manufacturing processes, as some processes involve the modification of metals (e.g., laser bed powder fusion and electron beam melting). Furthermore, many processes involve melt pools (LPBF and EBM), fluid droplets (material jetting), and other dynamic, non-opaque, and non-diffuse entities, continuously monitoring the size and shape of which could provide insight into the process or the final product. However, it is difficult for structured light-based systems to image because of their brightness, reflectivity, and non-opaqueness. The dynamic nature of these processes can also make it difficult for SLS systems to handle accuracy. Motion-induced errors occur when the measurement speed is less than the object's speed in motion [65]. Three-dimensional monitoring of complex structures, such as those created by material extrusion, can be challenging because of occlusion and the subsequent presence of shadows. Additionally, structured light systems are sensitive to

ambient light, and in the case of manufacturing processes that involve varying ambient lighting and radiation, whole-process monitoring can be difficult to achieve with structured light. Many additive manufacturing processes also involve closed chambers, which can make it difficult to fit in multi-camera projector-based SLS monitoring systems.

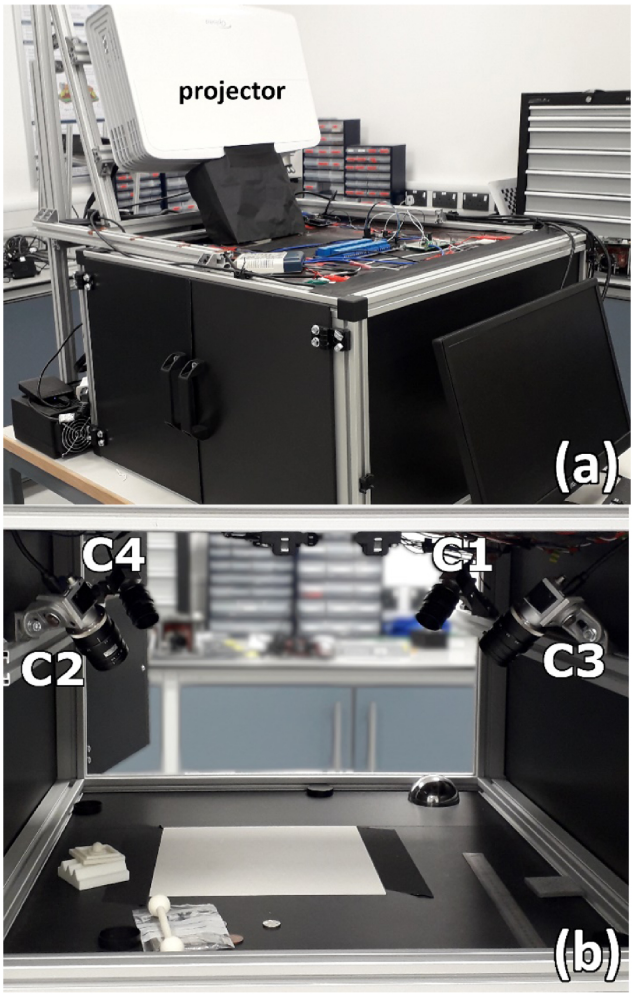


Figure 12. External (**a**) and internal (**b**) view of a four-camera fringe projection system installed inside a mock powder bed fusion chamber with cameras labeled C1 through C4 (reused from [66]).

4.4. Optical Coherence Tomography

Optical coherence tomography (OCT) is one of the widely used non-invasive imaging methods in the ophthalmology field [67]. OCT uses light waves to scan the object [68,69]. A typical OCT setup includes a light source (A), beam splitter (B), and interferometer (C) (detector). The schematic of OCT is illustrated in Figure 13. The light source emits a broad-band width light. This light is split by the beam splitter into reference and sample beams. The sample beam is reflected when striking the surface of the object. The reflected sample beam is recorded by the interferometer. The depth information is obtained by estimating the path difference between the reflected sample beam and the reference beam. There are different types of OCT, such as time domain OCT, spectral domain OCT, and time-encoded frequency domain OCT. It is extensively used for diagnosis in ophthalmology applications [70]. Similar to laser scanners, OCT technology is also well-commercialized [71]. Figure 14 shows the layout of an at-line mid-infrared OCT system for the inspection and quality assurance of additively manufactured ceramics. The main advantage of OCT is its high-depth resolution [72]. However, the scanning process is time-consuming compared to the other methods (DIC, laser scanner, and structured light). This makes it difficult to

successfully use in real-time 3D monitoring of additive manufacturing processes. Furthermore, OCT also suffers from saturation and occlusion errors, which makes it difficult to monitor additive manufacturing processes such as extrusion and powder bed fusion.

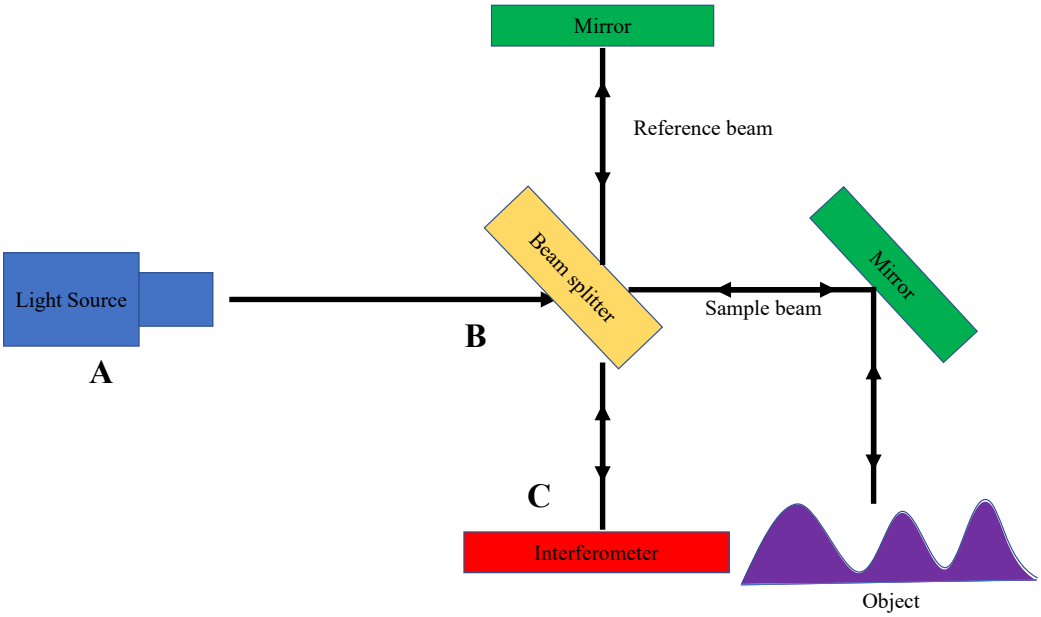


Figure 13. Schematicof OCT, consisting of a light source (A), beam splitter (B), and interferometer(C).

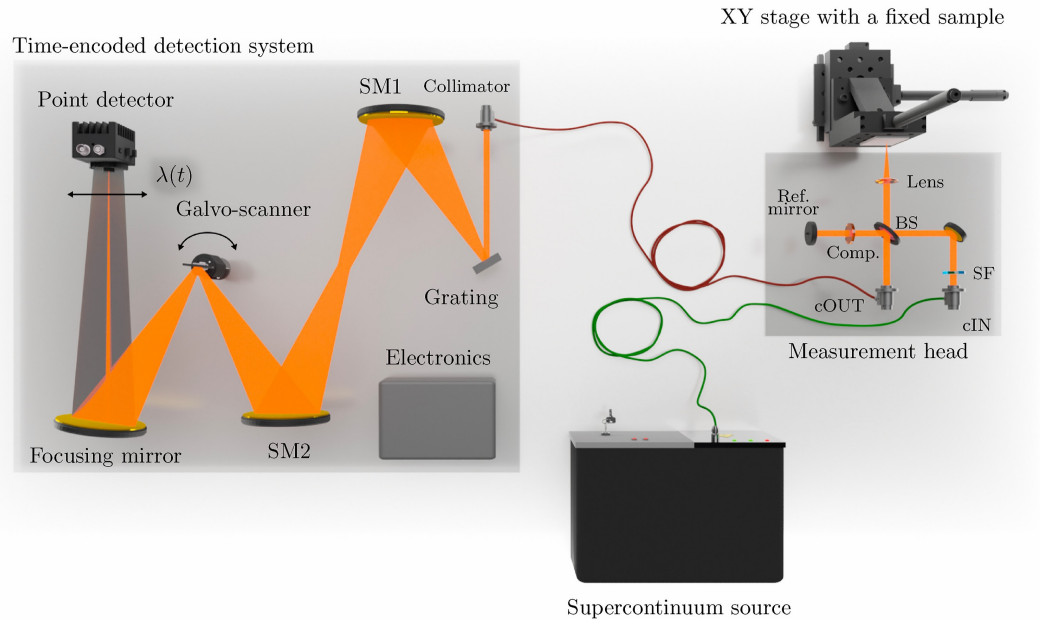


Figure 14. Layout of an in-line mid-infrared OCT system for inspection and quality assurance of additively manufactured ceramics (reused from [73]).

4.5. Data Processing and Analysis

In each of these monitoring techniques, data are collected in the form of a series of 2D images acquired at high speed. These images are then utilized to reconstruct a 3D profile of the object. This 3D profile is used in conjunction with machine learning frameworks for automated defect detection. Parameters like surface roughness can also be computed from its 3D profile and, with the help of machine learning/reinforcement learning-based frameworks, can be used to aid in defect detection and correction using closed-loop feedback control of process parameters. The data processing method differs

for each of the surface monitoring methods. Digital image correlation calculates surface deformations by correlating black and white speckle patterns in the captured images. Bartlett et al. [74] used 3D-DIC for the in situ monitoring of the direct metal laser sintering process. The captured speckled images were processed using a commercial DIC software (Vic-3D)to extract the surface profile of the powder bed and perform noise removal and anomaly detection. Finally, a naive Bayes classifier was used for defect classification. The entire workflow is illustrated in Figure 15.

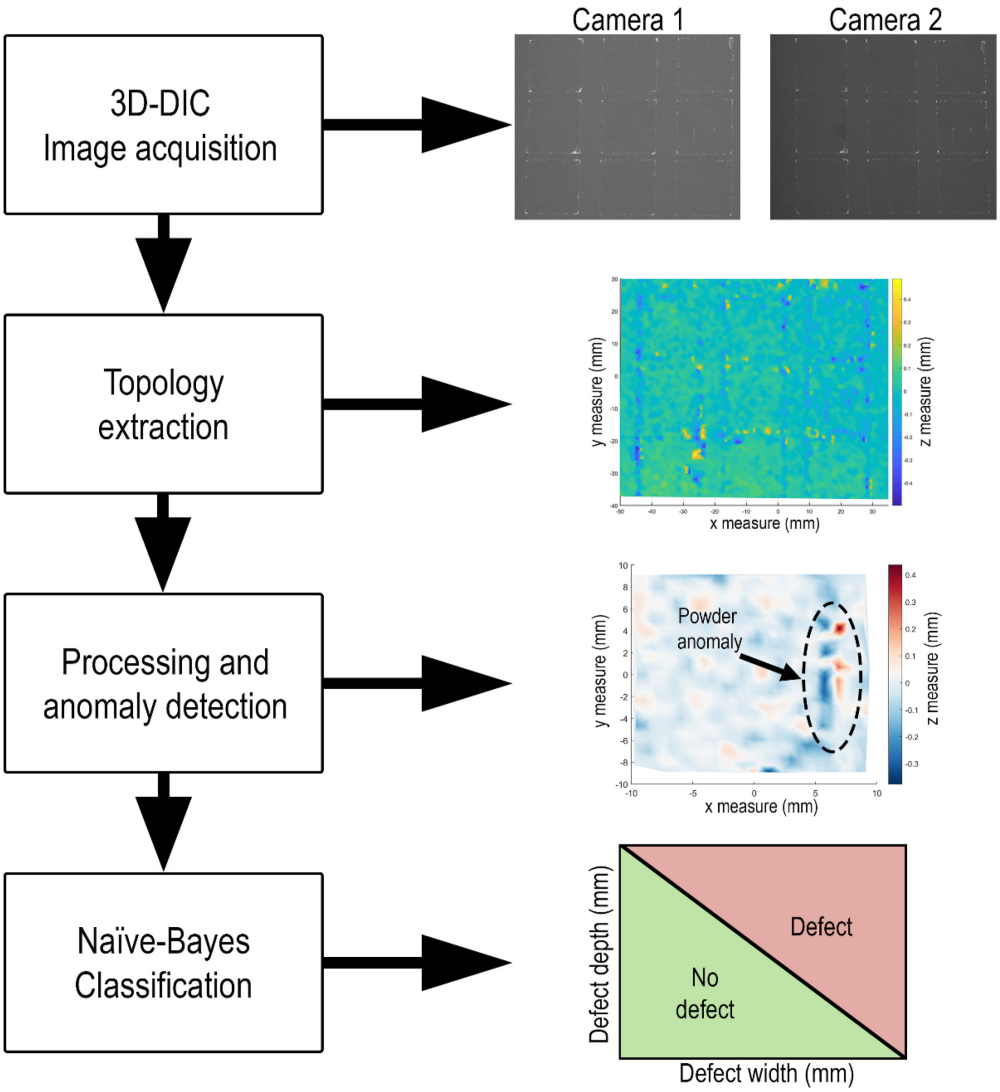


Figure 15. Sample data processing and analysis pipeline of digital image correlation for direct metal laser sintering (reused from [74]).

Laser scanning captures 3D point clouds of printed layers using laser sensors. As a representative example, Ma et al. [75] used laser-based 3D monitoring for an extrusion-based silicon AM process. Using the reconstructed 3D data, they standardized and segmented point clouds of each layer to subsequently extract cross-sectional width and height data, and clustering algorithms were used to filter out noise. They used the deviations in strand geometry to modulate feed rate and trajectory changes in subsequent prints. Similarly, Williams et al. [76] integrated a laser displacement sensor into the build chamber of an LBPF machine and continuously monitored the height profile of the part being built. Using the acquired depth information, they were able to compute the layer thickness and evaluate its behavior based on varying processing conditions. Figure 16 shows the plot of the position of the top surface layer across three layers during the first 400 layers of the

build. We can also see signatures associated with process events in Figure 16. The authors were able to identify a characteristic signature for key events in each layer, which allows the system to detect any variations in these signatures, underscoring the usefulness of this monitoring setup.

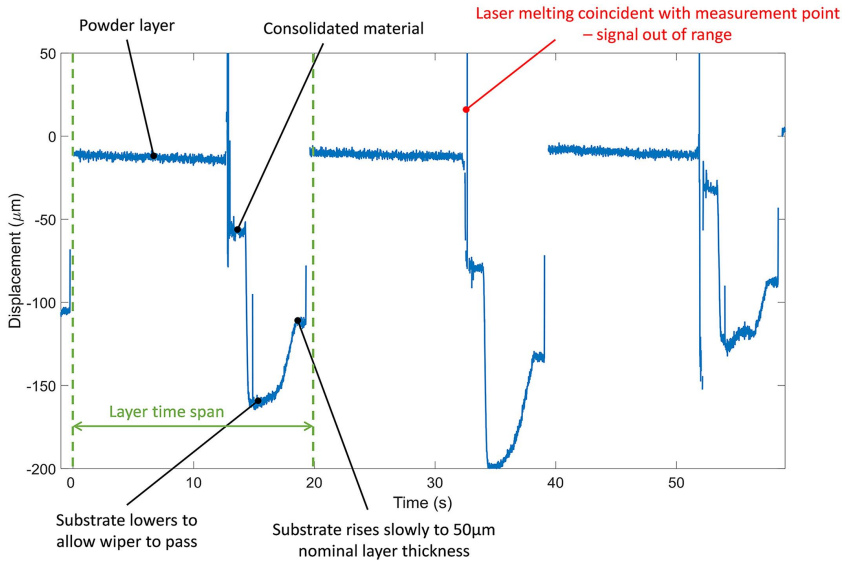


Figure 16. Sample data processing and analysis pipeline of the laser scanning system for laser powder bed fusion (reused from [76]).

Structured light systems involve the capture of black and white fringe-patterned images of the printed layer. Dickins et al. [66] integrated a multiview fringe projection system into a metal powder bed fusion setup and compared the results to the 3D profile obtained from a commercial focus variation (FV) microscopy system. Fringe projection systems produced 3D point clouds, while focus variation (FV) generated gridded height maps, with fringe projection covering a significantly larger field of view. Both datasets were cropped to isolate the sample's top surface, and fringe projection data were converted to height maps for direct comparison. Five repeated measurements from each system (single-/multi-view fringe projection and FV) were collected without sample repositioning, enabling the statistical assessment of measurement repeatability. Figure 17 outlines the processing pipeline used by the authors. Point clouds from each camera were processed in CloudCompare for initial cropping and statistical outlier removal. The data were then transferred to Polyworks | Inspector for manual refinement of the region of interest (RoI). A two-stage alignment process (coarse followed by fine) aligned fringe projection data to FV measurements.

Optical coherence tomography (OCT) is a non-destructive imaging technique that uses low-coherence infrared light to generate high-resolution, real-time 3D images of surface and subsurface features. Gardner et al. [77] used OCT to perform in situ process monitoring for the selective laser sintering process. Their data processing workflow involved two image processing phases to improve the signal-to-noise (SNR) ratio. Second-order interleaving was used to take every second datapoint in each A scan fringe to form two A scan fringes and average them out to improve the SNR. After this step, the contrast was adjusted, and a block-matching 3D filter was applied. The second phase corrected for the effects of field curvature, and the final step involved depth detection, wherein the top and bottom surface of the melt pool were detected by edge detection algorithms, and the melt pool depth was calculated by the mean distance from the top surface, and the excessive heat error was recorded as the max distance of the melt pool edge from the melt pool mean depth. This process is illustrated in Figure 18.

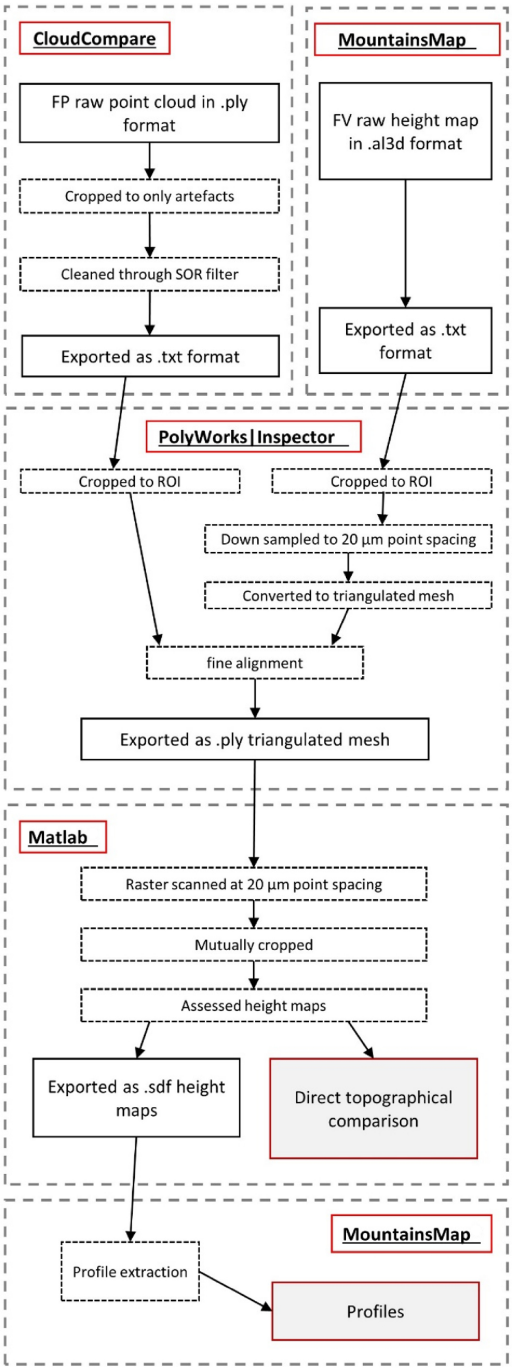


Figure 17. Sample data processing and analysis pipeline of structured light-based in situ monitoring system for metal powder bed fusion (reused from [66]).

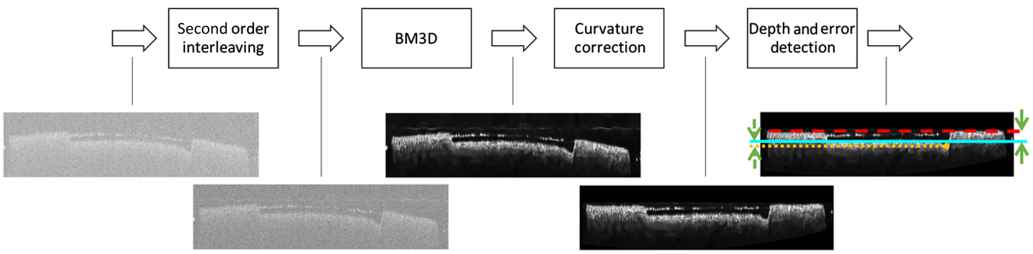


Figure 18. Sample data processing and analysis pipeline of the OCT monitoring system for selective laser sintering, with the red dashed line denoting the upper surface of the melt pool, the blue line denoting the lower surface of the melt pool, and the yellow dotted line denoting the excessive heat error (reused from [77]).

5. In Situ 3D Surface Monitoring Technologies for Additive Manufacturing

Over the years, researchers have successfully built and integrated 3D shape measurement methods with various additive manufacturing processes for in situ surface topography monitoring. We have classified research based on the additive manufacturing process into four categories.

5.1. In Situ 3D Monitoring for the Powder Bed Fusion Process: Current Practices and State of Closed-Loop Feedback Control

In situ 3D monitoring techniques for powder bed fusion (PBF) processes have emerged as critical tools for ensuring part quality and process reliability. While significant advances have been made in implementing various sensing modalities like structured light-based imaging, laser scanning, and optical coherence tomography for real-time process monitoring, several challenges remain in achieving robust closed-loop control.

5.1.1. Current Practices: In Situ 3D Surface Monitoring for PBF

Table 2 provides a comprehensive summary of the different in situ 3D monitoring methods for the powder bed fusion process. Foster et al. [78] developed a surface topography monitoring method for a metal powder bed fusion additive manufacturing process (PBFAM). The authors classified the defects in the PBFAM process into three categories: (i) defects caused by machine parameters, (ii) defects caused by the build plan, and (iii) defects due to improper calibration and equipment damage. Among these, the focus was to identify the defects caused by the build plan. These defects included the variations in part geometry caused by changes in thermal gradient and distortion. The authors used a pseudo 3D imaging method, i.e., 2D images of the build layer were captured (after each layer of printing), and the 3D model of the printed part was obtained by stacking the images. The authors designed a part-build plan with intentional defects to evaluate their monitoring system. The system setup included a high-resolution camera that captured images after the recoating process and the laser exposure. The 3D model was obtained by stacking the 2D images captured at each layer. From the 3D model, the layer at which the defect occurred was visually identified. However, the authors only used the 3D data for visualization purposes, and no analysis was performed. Moreover, the 3D model was a combination of different 2D images, making it difficult to identify the internal defects in each layer. Williams et al. [76] used a laser scanner to monitor the process signatures of a laser powder bed fusion process (LPBF). The authors integrated a Keyence laser displacement sensor into the build chamber of a laser bed powder fusion machine, monitoring the height of the top surface layer to measure the layer thickness and characterizing the effect on it with respect to a change in processing conditions. The authors visually tracked surface parameters such as layer height and process signatures from the 3D topography data. However, the surface scanning process is time-consuming.

Table 2. Comprehensive summary of the different in situ 3D monitoring methods for the powder bed fusion process.

Article	Year of Publication	Three-Dimensional Monitoring Technology	In Situ Monitoring	Features Extracted	Precise Metrology	Closed-Loop Feedback Control	Accuracy of the Three-Dimensional Monitoring System
Williams et al. [76]	2021	Laser scanner	Yes	Layer height	No	No	Not Measured
Dickins et al. [66]	2020	Structured light	No	None (topography was visualized)	No	No	Not Measured

Table 2. *Cont.*

Article	Year of Publication	Three-Dimensional Monitoring Technology	In Situ Monitoring	Features Extracted	Precise Metrology	Closed-Loop Feedback Control	Accuracy of Three-Dimensional Monitoring System
Southon et al. [79]	2018	Structured light	Yes	Surface curling, irregularities, and powder spreader blade interactions	No	No	Stated volumetric accuracy of 15 µm after calibration
Zhang et al. [80]	2022	Structured light	Yes	None (topography was visualized)	No	No	12.01 µm across powder surface and 19.23 µm across printed surface
Zhang et al. [81]	2023	Structured light	Yes	Height maps	No	No	RMSE of 4.35 µm
Land et al. [82]	2015	Structured Light	Yes	None (topography was visualized)	No	No	18 µm in the vertical measurement
Liu et al. [83]	2020	Structured Light	Yes	Thermal swelling (resulting in an increase in the average height of the topography)	No	No	15.8 µm
Zhang et al. [84]	2016	Structured Light	Yes	Splatter and height variations in the printed layer	No	No	0.47 µm
Kalms et al. [85]	2019	Structured Light	Yes	Height variations caused by surface irregularity	No	No	10 µm
Li et al. [86]	2018	Structured Light	Yes	Surface contours and height variations in the surface	No	No	Not Measured
Remani et al. [87]	2024	Structured Light	Yes	Surface roughness parameters	No	No	Not Measured
Liu et al. [88]	2021	Structured Light	Yes	Edge thermal swelling and surface depressions	Yes	No	15.8 µm
Kanko et al. [89]	2016	Inline coherent imaging	Yes	Height map and melt pool depth	No	No	Not Measured
DePond et al. [90]	2018	Spectral domain OCT	Yes	Surface patterns, geometry, profile thickness, and surface roughness	No	No	Not Measured
Guan et al. [91]	2015	OCT	No	Voids, surface roughness, and fewer solidified regions	No	No	30 µm
Lewis et al. [92]	2016	OCT	Yes	Curls on the surface	Yes	No	Not Measured
Gardner et al. [77]	2018	OCT	Yes	Curls on the surface, melt pool depth (solidification behavior), and surface irregularities caused by excessive heat	Yes	No	Not Measured

Eschner et al. [93] built a stereoscopic system (two cameras) to monitor the LPBF process. The authors primarily focused on tracking the powder particles. This is essential

because these particles might be melted and form spatters, leading to fusion defects on the printed layer. The monitoring setup consisted of two cameras with an illumination source. Their method had three steps: (i) identifying the particles in the camera image, (ii) performing correspondence matching on the two camera images, and (iii) estimating the 3D coordinates of the particles. In order to increase the robustness of the correspondence-matching process, the authors used a priori information with a Kalman filter [94], with which the position of the particles in the previous frame was obtained. The authors verified their method by conducting a simulation experiment where particles of known velocity and trajectories were made to move in a 3D volume. The measurement error increased when the number of particles increased. The main limitation of this approach is that it did not analyze the quality of the printed layer; rather, the particle movement was studied. Moreover, the method might not accurately estimate the position of the particles in the 3D space as it relies on the particle's pixel intensity for performing the correspondence match.

Dickins et al. [66] compared multi-view and single-view fringe projection methods to measure the surface topography of a powder bed fusion system and showed that the multi-view system was less precise but more accurate with higher surface area coverage than a single-camera system. The authors used a multi-view fringe projection system, which consisted of four fringe projection systems arranged circularly to aid visibility in areas that were not accessible by a single fringe projection system. The point clouds from the different systems were stitched, and the accuracy was evaluated by comparing the topography with that of a high-resolution system (a focus variation microscope). However, monitoring was conducted ex situ. Southon et al. [79] investigated the feasibility of using fringe projection to monitor the powder bed of a polyamide 12-polymer laser sintering machine. They identified a number of defects, such as curls, surface irregularities, powder spreader blade interactions, and structural defects during the printing process using fringe projection by recording the 3D structure of the powdered bed after each layer was printed. The defects had a wide size range, from hundreds of micrometers to hundreds of millimeters. However, the monitoring system was not fully integrated into the printing chamber, which increased the time needed for the entire build process. Due to its competency in detecting catastrophic structural defects, FPP can potentially be part of a feedback and control system that interrupts the build and corrects for in-process defects where possible. One limitation to this is the fact that polymer degradation occurs before curling at optimal temperatures, one of the major defects that FPP is able to detect in this process. This makes it difficult to establish a one-to-one link between curling and the final material properties and makes it hard to determine the right point and necessity of intervention. Zhang et al. [80] developed a cost-effective and non-invasive technology to measure finer features specific to the LPBF process. They developed an in situ FPP method to measure the dynamic topography of the powder bed and printed layer during laser powder bed fusion. Their FPP method is specific to LPBF systems because of their implementation of pixel-wise correction functions that capture the effects of measured location-induced light propagation path difference, surface reflectivity non-uniformity across the powder bed, and sensor non-linearities. The system's accuracy was evaluated by comparing the 3D topography with the corresponding topography measured using a Keyence microscope. However, the 3D topography was not analyzed for any potential defects in the printing process. The same research group [81] developed a machine-learning model to improve the accuracy of the 3D topography of samples estimated by the fringe projection system in an LPBF process. The authors focused on two parameters: (i) saturation (caused by highly reflective regions) and (ii) resolution. The authors developed a high dynamic range method similar to Suresh et al. [95] to resolve the saturation while performing 3D scanning. To improve the resolution, a deep learning model was developed. The model was trained to transform the height maps from the

fringe projection system to a high-resolution height map (16 X) (similar to an optical microscope). However, the authors did not further analyze the high-resolution topography data. Land et al. [82] explored the feasibility of in situ monitoring of the LPBF process using a digital fringe projection system. Two systems were used: (i) digital fringe projection for obtaining the height profile of the printed layer and (ii) a machine vision system for obtaining the planar image of the printed layer. The two system setups included a projector and multiple cameras. The planar coordinates of the printed layer were obtained from the machine vision system (a single-lens reflex camera). The surface profile was measured using the two systems before and after the laser exposure. The planar coordinates and the height map were combined to obtain the 3D point cloud data. They were able to achieve a noise floor of 18 μm, allowing recognition of sintered area depths and surface features. However, the authors were not able to image all steps and layers in the build process and additionally did not perform any interpretation of the 3D data. Moreover, the system setup may have some redundancies as the planar information could also be obtained from the fringe projection system.

Liu et al. [83] developed an in situ inspection method using a fringe projection system for monitoring the electron beam melting (EBM) process based on the enhancement of a single-view fringe projection technique using a novel surface fitting technique. Surface fitting was used to enhance the calibration process and mitigate the phase and measurement errors arising from low fringe contrast due to the presence of black circle rings on the calibration board. The authors built three prototypes (an in situ monitoring setup) to validate the reliability and to perform in situ monitoring. The first prototype involved a simulation experiment to evaluate the system's robustness. The second prototype was used to evaluate the accuracy of the system. The third prototype was integrated with the vertical translation stage of the EBM machine. Upon deployment, this system was able to achieve a vertical resolution below 20 μm and a standard deviation of around 15.8 μm on a flat plane. The 3D geometry of the powder bed was measured using the fringe projection system after each layer of printing. The powder height increased at certain layers because of thermal swelling. If the powder height was above a certain threshold, the building process was stopped, and the operator was informed. The build process only resumed when the powder surface was sufficiently smooth. However, the inspection system was only used to make a binary decision of whether the powder height was below the acceptable threshold; other forms of surface deviation (such as pores) were not analyzed.

Liu et al. [88] developed an intelligent fringe projection system with a support vector machine (SVM) algorithm for in situ monitoring of electron beam additive manufacturing processes, enabling simultaneous measurement of both reflective solidified metal surfaces and diffuse powder beds. The system achieved a recognition rate exceeding 91 for printed samples and reduced measurement time from 16 s to approximately 4 s compared to traditional multi-exposure methods. It was successfully implemented in a commercial EBM machine and demonstrates the capability to detect common defects such as edge thermal swelling and surface depressions during the build process.

Zhang et al. [84] used a fringe projection system to monitor the surface topography of the LPBF process, including powder bed signatures such as powder layer flatness, surface texture, the average height drop of the fused regions, characteristic length scales on the surface, and splatter drop location and dimension. The authors developed a reference-based phase unwrapping method for the fringe projection system. The process monitoring involved measuring the build layer at two stages. The 3D geometry of the bed surface was measured after each layer of powder spread and after laser fusion. The first measurement was used for monitoring the surface flatness and the height consistency of the powder on the layer, whereas the second measurement was used to analyze the height variations in the

build. The stability of the process was monitored by observing the average height difference between the fused and unfused regions. A model based on arithmetic progression was used to predict the average height drop of the build. According to this, the average height drop at a layer is defined as follows:

$$h_n = -t\alpha * \left\{ \frac{1-\alpha^n}{1-\alpha} \right\}, \quad (1)$$

$$\alpha = 1 - \beta, \quad (2)$$

$$\beta = \frac{powder\ density}{metal\ density}, \quad (3)$$

where h_n is the average height drop at a layer, t denotes the powder layer thickness, and β is the shrinkage ratio. The splatters (high spots in the unfused regions) were also identified from the measurements taken after the laser fusion. This method analyzed various surface parameters such as flatness, height variation, and splatter from the measured 3D surface profile. However, the limitation is that the system requires precise adjustment of illumination levels for each layer as there might be saturation on the metal surface, which will result in incorrect depth estimation in those regions. Kalms et al. [85] developed a surface profile monitoring method using a dual-camera structured light system for the laser beam melting process. Three synthetic wavelengths, each with a four-step phase-shifted fringe pattern, were used to obtain the phase information. The surface of the printed layer was measured before and after powder deposition. Irregularity in the feed was identified from the height maps obtained from the reconstructed 3D data. The authors conducted an experiment involving a damaged layer. The damaged layer caused a non-uniform powder arrangement, leading to irregularity in the printed layer. This was validated by the surface measured by the structured light system. The authors demonstrated that the vertical accuracy of the system was less than 10 µm, making it suitable to reliably detect errors in powder coating or consolidation at a layer thickness of 50 µm. The main limitation of this method is the measurement speed, as it involves four- or higher-step phase-shifted fringe patterns for phase estimation. Such a setup might make it difficult to monitor the printing process in real time.

Remani et al. [87] developed and validated a novel in situ monitoring approach using fringe projection for laser-based powder bed fusion, enabling layer-wise surface topography measurements during the build process. The system consisted of a single-view fringe projection setup integrated into a commercial LPFB machine, capturing post-melting layer measurements through automated triggering. The researchers proposed and validated nine custom topography indicators computed from the fringe projection data, with five indicators showing z strong correlation with final part quality as verified through X-ray computed tomography (XCT) density measurements. Statistical process control methods using X-bar control charts demonstrated the system's capability to detect quality variations induced by laser defocusing, particularly through indicators such as mean height in processed regions and height kurtosis in unprocessed regions.

Li et al. [86] used a dual-camera structured light system to monitor two types of geometric patterns (3D surface geometry and 3D contours of the fused region) of the parts made by the powder bed fusion process. Specifically, the authors developed two methods: (i) enhanced phase-shifting profilometry and (ii) slice model-assisted contour detection for monitoring the geometric patterns.

Using enhanced phase-shifting profilometry, 3D reconstruction was performed using three fringe images. The method was validated by performing a fusion process with defects, leading to a height change in the printed layer. The change in the average height of the build was observed on the 3D surface, and the cross-sectional profile obtained

from the measured 3D confirmed the height difference. The slice model-assisted contour detection method involves identifying contours from camera images. However, unlike the previous method, the authors used a stereoscopic system for 3D reconstruction of the identified contour regions. The contour map was refined in an iterative process by using the computer-aided design model (CAD). The refined contour map was used for 3D reconstruction. The method was validated by obtaining the 3D contour data of the layers printed with intentional defects. However, no further analysis was performed using the 3D data apart from monitoring the average height. Another limitation associated with the fringe projection systems is the resolution; it is limited to a few 100 µm for a macroscopic system [64].

High volumetric resolutions can be achieved with the help of the optical coherence tomography (OCT) method. Kanko et al. [89] demonstrated the feasibility of the spectral domain optical coherence tomography (SD-OCT) method in monitoring the LPBF process. The authors used an inline coherent imaging (ICI) method, which is similar to SD-OCT. They conducted several experiments to monitor the melt pool depth and analyzed the impact of various laser powers, powder thickness, and processing overhang structures. The repeatability of ICI was also evaluated. By analyzing the melt pool stability, the defects were identified. However, the research was limited to single-dimensional printing, and ICI's potential for multi-dimensional printing was not explored. DePond et al. [90] used an SD-OCT technique to monitor the height variations in the LPBF process. From the SD-OCT scans, the surface roughness, surface pattern, and profile thickness were estimated. However, the vertical resolution of the system was limited by the coherence of the light source, and the lateral resolution was limited by the diameter of the laser beam. Guan et al. [91] developed a 3D surface monitoring method using OCT for a selective laser sintering process. OCT scanned the surface of the polymer parts printed by the laser sintering process. The authors estimated surface roughness, dimension of open voids in the printed layer, and solid and loose sintered areas from the topography obtained from OCT scans using signal attenuation as a function of depth. However, most of the measurements were ex situ. Lewis et al. [92] explored the potential of OCT in performing in situ 3D topography measurements for a laser additive manufacturing pilot system. The authors used a swept-source laser OCT setup. The scan area was marked on the build surface by two holes spaced 4 cm apart. An OCT scan was performed before and after the laser sintering process in the scan area. The scanning process had two outcomes: (i) an A-scan,i.e., an OCT scan taken at a single point on the sample, and this has the depth information of that point, or (ii) a B-scan, i.e., a collection of multiple A-scans, which provides a 3D representation of the entire surface. In this research, the authors built a B scan by combining 512 A scans, and each A-scan had a high axial resolution of 3.75 µm. Because of the low signal-to-noise ratio, the OCT scans were denoised before analyzing for any surface variations. However, it was difficult to differentiate between the sintered layers and unsintered powder from the B-scans due to the less powerful OCT. The same research group [77] performed various experiments using different laser powers to establish a correlation between laser power and surface defects on manufactured parts. The authors proposed a new method called second-order interleaving to improve the signal-to-noise ratio of A scans. This process involved separating the odd number data points and even number data points from the A scan and averaging the two data point sets. Following this, the A-scans were denoised by a block-matching, three-dimensional filter [96]. Two parameters were observed from the B-scans: (i) melt pool depth, i.e., the mean distance from the top surface to the bottom surface, and (ii) excessive heat error, i.e., the maximum distance of the melt pool edge from the melt pool mean depth. Both parameters increased with an increase in laser power. However, the major limitation of this approach is the field of view, which is an approximately

45 mm-radius circle. Moreover, the OCT system cannot monitor an additive manufacturing method in real time.

5.1.2. Current State of Closed-Loop Feedback Control for PBF Based on In Situ 3D Surface Monitoring

Closed-loop feedback control in laser bed powder fusion has been a difficult task for researchers to achieve. This is due to multiple reasons. Firstly, the laser speed in the LPBF process is blazingly fast, upwards of a thousand millimeters per second, which requires a sensing speed of greater than 1 kHz. This implies that data acquisition, information transfer, and data processing combined must be capable of real-time feedback, which is difficult to achieve [97]. Secondly, closed-loop control involves defect detection and the ability to immediately correct and mitigate further defects and achieve target material properties. However, it is sometimes difficult to establish a one-to-one link between a defect detected in the process and its impact on the final material properties. Southon et al. [79] demonstrated the capability of FPP in detecting defects in the laser sintering process. FPP was able to detect curling, which was a catastrophic defect that occurred during the process. However, polymer degradation occurs before curling at optimal temperatures, which makes it hard to establish a link between the defect and the final material properties. Thirdly, the LPBF process inherently involves some randomness; droplet spreading and powder spreading quality are highly random, and this stochastic and dynamic process poses challenges to modeling a closed-loop control system.

Laser power is the most appropriate parameter for real-time control in the LPBF process because it can be controlled directly and independently. Fixed laser power, regardless of raster length, will cause quality issues such as sharp corners due to heat accumulation, high surface roughness due to insufficient melt, and dents and swellings due to excessive power; therefore, this is an important parameter to control. Wang et al. [97] used high-speed thermal sensing to control laser power in real time. Vasileska et al. [98] used a layer-wise control method, lowering the laser power to compensate for the over-melt of the previous layer. Shkoruta et al. [99] used an image-based control method to regulate the laser power in LPBF. These methods are fairly simplistic and also rely on the modification of laser power as the only parameter in the closed-loop control process.

The current state of process monitoring in this field revolves predominantly around layer-by-layer monitoring. Montazeri et al. [100] monitored the LPBF process with a photodetector in order to detect material cross-contamination by monitoring photodetector sensor signatures hatch by hatch. Guerra et al. [101] used a high-resolution optical tomography technique to monitor the LPBF process layer by layer and successfully detect geometric distortions in the LPBF process. Whole-process monitoring in LPBF is not as common, but a few existing approaches focus on data from one sensing modality. Gaikwad et al. [102] were the first to use multiple cameras; they used two co-axial high-speed thermal video cameras and a temperature field imaging system to monitor the melt pool stage of the laser bed powder fusion process and were among the first to adopt a data fusion approach to capture these phenomena. Melt pool temperature, shape and size, and spatter intensity were extracted from these data and used to train a machine-learning model to detect laser defocusing and predict porosity type and severity. Zou et al. [103] used a high-speed camera with a 10 kHz sampling rate to acquire images of the melt pool phase, using image processing techniques to extract the melt pool width, length, and area, fusing them with light-intensity signals from three silicon photodiodes, and feeding this as an input to a convolutional neural network in order to classify defects of sizes ranging from 100 to 500 micrometers.

Machine learning has been proposed as a possible method to facilitate fully autonomous feedback control [104,105], but researchers have not been able to implement a

complete ML-based closed-loop implementation to facilitate a fully autonomous process that can course-correct defects yet. Future research should focus on developing robust ML algorithms capable of real-time process monitoring and adaptive control strategies to enable autonomous defect correction in closed-loop LPBF systems.

5.2. In Situ 3D Monitoring for Direct Energy Deposition Processes: Current Practices and the State of Closed-Loop Feedback Control

Direct energy deposition (DED) is an additive manufacturing technique that enables rapid fabrication of metal components, yet faces challenges with residual stresses and non-uniform heating that can lead to deformations and defects. In situ monitoring systems have emerged as critical tools for real-time quality control and process optimization, employing various sensors and imaging techniques to track melt pool dynamics, thermal distributions, and structural deformations during fabrication.

5.2.1. Current Practices: In Situ 3D Surface Monitoring for DED

Table 3 provides a comprehensive summary of the different in situ 3D monitoring methods for the direct energy deposition process. Heralic et al. [106] developed a 3D topography monitoring method using a laser scanner for the laser metal wire deposition process. The authors used a commercial 3D scanner (Micro-Epsilon), which has a depth resolution of 10 µm. The scanner was attached to the drive unit. The authors used an iterative learning control method [107] to achieve a uniform deposition at each layer and to maintain an even layer height. The monitoring process involved scanning each layer after deposition using the laser scanner. An error term was calculated based on the current layer's height (obtained from the 3D scanner) and the mean height of the part. This error term is used in the iterative learning control algorithm to alter the feed rate for the next build in order to achieve a uniform height by compensating for the errors that occurred in the previous layer. The authors validated their method by building a cylindrical object. The overall build was observed to have an even height except for the outer layer of the cylinder. This was mainly because the 3D scanner could not estimate the cylinder's depth information at the boundary because of saturation in the outer region. Moreover, the authors used a single exposure time for the entire scanning process, resulting in incorrect depth estimation at highly reflective regions on the cylinder. Tang et al. [108] also used a laser scanner for topography repair in a wire arc additive manufacturing process. The monitoring method involved obtaining the 3D topography of each layer after the deposition process. The 3D point cloud data were converted to a 3D depth image. From this depth image, various features (defects) were segmented by a threshold process. The threshold was defined by the pixel intensity. The contours of the features were obtained by inverse one-to-one mapping and sliced into a set of 2D layers. Corresponding path-planning modules and G-codes were generated for material deposition in regions near the segmented feature in the next layers. As the method largely depends on the laser scanner's accuracy, the authors validated the scanner's accuracy by measuring the heights of standard blocks. The main limitation of this method is that the repair process is based on the regions segmented by pixel-based thresholding instead of estimating the deviations of the build part by comparing it with the CAD model.

Binega et al. [109] developed a process monitoring method for a direct energy deposition (DED) process by comparing the build layer with the CAD model. The authors used a laser scanner to obtain the 3D topography of the build layer. The process monitoring framework involved three steps: (i) in situ scanning of the built layer using the laser scanner, (ii) extraction of various geometric attributes from the 3D scan (the geometric attributes are illustrated in Figure 19), and (iii) plotting and comparison of the actual design model with the built model. The laser scanner was attached to the nozzle of the DED

machine, and the topography was scanned after each build. The coordinates of the 3D point cloud obtained from the laser scanner were transformed to a global coordinate system, and the transformed 3D data were compared with the actual design model of the part. The geometric parameters (as defined in Figure 19) of the design model and build model were plotted in a graphic user interface (GUI). The authors evaluated their method by conducting two experiments: (i) single-layer and (ii) multi-layer metal track object printing. The authors also evaluated the efficiency of the in situ monitoring method by scanning the parts post-printing. The geometric attributes measured in situ varied significantly from the post-printing measurements. This was attributed to the powder spreading and changing light conditions. However, the main limitation of this method is the time taken to complete a full surface scan. The laser scanner uses a line of laser light to recover the depth information of the part. The scanner has to move across the entire surface of the part to obtain a full surface scan. This process might be time-consuming and might delay the build process.

Table 3. Comprehensive summary of the different in situ 3D monitoring methods for direct energy deposition processes.

Article	Year of Publication	Three-Dimensional Monitoring Technology	In Situ Monitoring	Features Extracted	Precise Metrology	Closed-Loop Feedback Control	Accuracy of the Three-Dimensional Monitoring System
Heralic et al. [106]	2012	Laser scanner	Yes	Layer height	No	Yes	Not Measured
Tang et al. [108]	2019	Laser scanner	Yes	Surface deviations from the CAD model	Yes	Yes	Average error of the system is between 0.02 mm and 0.07 mm
Binega et al. [109]	2022	Laser scanner	Yes	Track width, deposition height, and discrepancy area	Yes	No	Overall RMSE error of deposition height is 0.028 mm and overall RMSE of track width is 0.133 mm
Zhang et al. [110]	2021	Structured light	Yes	Defects such as holes	Yes	Yes	Not Measured

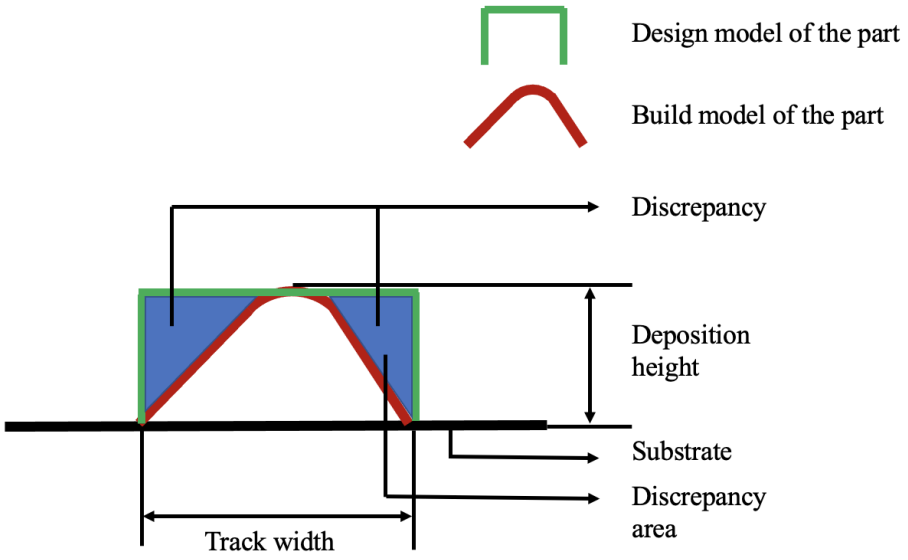


Figure 19. Geometric attributes measured from the 3D scan.

Zhang et al. [110] used a structured light system for guiding the DED machine in repairing defective parts. The authors integrated the structured light system inside the DED machine to monitor the build process. The method involved scanning the defective part using the structured light system. The milling depth was estimated from the 3D scan (depth of the defective part). The G-code for the machine was generated using the milling depth information. After the completion of the repair, the final part was evaluated for internal pores using a computerized tomography scan [10]. The authors evaluated this repair framework on a defective engine head. However, the 3D topography from the system was not used for dynamically modifying the build process through a closed-loop method. Instead, it was only used at the beginning of the build process.

5.2.2. Current State of Closed-Loop Feedback Control for DED Based on In Situ 3D Surface Monitoring

As demonstrated by Heralic et al. [106], Tang et al. [108], and Zhang et al. [110], closed-loop feedback control using 3D monitoring has been successfully achieved and implemented in this domain. However, these researchers implemented layer-wise control, wherein the measurement from each layer was recorded and used to modify the input for the next layer.

Real-time feedback control was also achieved by researchers in this domain. However, most of the research works predominantly focused on modifying laser power using a controller to change the geometrical parameters of the melt pool.

For example, Akbari et al. [111] monitored the DED process in real time using a camera with an infrared filter and modified laser power using an adaptable proportional-integral (PI) controller to ensure constant melt pool width. They used 2D imaging, in combination with image processing techniques such as binary thresholding, and applied image filters to measure the melt pool width in real time, which was then used to modify the laser power depending on its difference from the user's set point. Gibson et al. [112] also used a thermal imaging system to monitor the direct energy deposition of Ti-6Al-4V and controlled the melt pool size by modifying the laser power using a closed-loop system. Superfast 3D imaging techniques such as structured light-based imaging could have easily been used in these scenarios and could perhaps have been used to study and control more geometrical aspects of the melt pool's 3D shape, as that would have an influence on the quality of the final product.

However, real-time, closed-loop feedback control that can facilitate a completely autonomous manufacturing process, ideally one that can control and modify a number of important process parameters and course-correct for possible defects on the fly, has not been achieved. This is due to challenges involving modeling the dynamic nature of the DED process, including the geometry of the dynamically changing melt pool and dynamics of material solidification, to gauge how they are impacted by process parameters such as laser power, material feed rate, particle diameter, powder density, and environmental factors. Additionally, due to the speed of the process, there is a need for extremely fast measurement acquisition. Data from high-speed 3D monitoring, which could provide copious amounts of real-time data on important geometrical process properties like the melt pool dimensions, melt pool accumulation, and possible defect occurrences, used in conjunction with machine learning could be an important step in the path to full process autonomy.

5.3. In Situ 3D Monitoring for Material Extrusion Processes: Current Practices and the State of Closed-Loop Feedback Control

Material extrusion is one of the most widely adopted additive manufacturing technologies, yet achieving consistent part quality remains a significant challenge due to process variations and environmental factors. Three-dimensional in situ monitoring systems have

become increasingly essential for this process to detect and measure critical parameters such as filament flow rates, layer adhesion, and geometric accuracy during the printing process.

5.3.1. Current Practices: In Situ 3D Surface Monitoring for Material Extrusion

Table 4 provides a comprehensive summary of the different in situ 3D monitoring methods for the material extrusion process. Li et al. [113] used a laser confocal displacement meter to monitor the quality of parts printed by a fused deposition molding process. Like the laser scanner, the laser confocal displacement meter should be moved across the entire printed layer to obtain the depth map of the layer. In this research, the authors treated the scanner as another printer head. Programmatically (using G-code), the scanner was made to scan after printing a layer of material. Various printing defects, such as shrinkage of printed layer and positional inaccuracies, were identified by comparing the 3D topography obtained from the scanner and the CAD model. However, the defect identification was carried out by visual inspection. Moreover, the scanning process was time-consuming, which, in turn, increased the time for the entire printing process. The same research group [114] developed a topography monitoring method using a laser scanner for a material extrusion process and a deep learning-based method to predict the print surface of a part given the CAD model. The topography monitoring method involved scanning the print surface after each layer of printing. The 3D point cloud data were transformed to a global coordinate system using the iterative closest point (ICP) algorithm [115] for comparison with the point cloud data of the reference CAD model. The geometric deviation was computed by estimating the difference between the two point clouds. The deep learning-based method involved training several conditional adversarial networks [116] to predict the topography of the printed part for a given reference CAD model. The accuracy of the model was evaluated by comparing the predicted topography with the topography obtained after scanning. However, the main limitation is that the geometric deviations were not incorporated into the printing process through a closed-loop feedback system. Armstrong et al. [117] developed a closed-loop monitoring system using a laser scanner for an extrusion-based bioprinting process. The laser scanner was attached to the extrusion head. After each layer of printing, the 3D topography of the surface was obtained from the laser scanner. From the 3D topography and the design model, the printing error was estimated, and the printing trajectory was modified accordingly to reduce the printing error. The laser scanner scanned the part after this correction process, and it was compared with the design model again to estimate the new error. This process was repeated in iterations. However, the main limitation is the time taken to scan the printed layer.

Nuchitprasitchai et al. [118,119] used a two-camera setup to monitor the material extrusion process and were able to create a system wherein if a defect was detected (where a defect is defined as greater than a five percent error between the 3D reconstructed image and the 3D printed product), an action was taken to stop printing.

Wi et al. [120] evaluated the quality of 3D clay samples using a structured light system. The 3D-printed clay samples were scanned by the structured light system. The printing quality was evaluated by extracting various surface parameters such as surface roughness, sample height, layer thickness, and surface angle from the 3D point cloud. However, the scanning process was carried out ex situ. Liu et al. [121] used a structured light scanner to perform in situ topography monitoring of honeycomb structures printed by the material extrusion process. The authors developed a modeling platform called the Mechanics of Structure Genome. The 3D scan obtained from the system was analyzed, and various structural properties, such as stress, plate stiffness matrix, etc., were estimated using this tool. However, there was no closed-loop control system for correcting the printing errors estimated using this tool. Moreover, the model was not tested on geometries other than

honeycomb structures. Girard and Zhang [122] presented a novel approach for accelerating error detection in additive manufacturing through structured light 3D imaging that minimized necessary reconstruction and comparison operations. Their method leveraged native pixel-by-pixel mapping between captured 2D images and reconstructed 3D point clouds, allowing error detection to be performed in the 2D phase domain prior to 3D point cloud generation. The technique demonstrated significant speed improvements compared to traditional methods based on global 3D reconstruction and point cloud processing, with speed improvement factors ranging up to 305 depending on the percentage of erroneous pixels. The authors validated their approach through experimental testing on a material extrusion system and implemented a closed-loop layer-wise error correction strategy, showing successful detection and correction of both single-layer and multi-layer geometric errors.

Table 4. Comprehensive summary of the different in situ 3D monitoring methods for material extrusion processes.

Article	Year of Publication	Three-Dimensional Monitoring Technology	In Situ Monitoring	Features Extracted	Precise Metrology	Closed-Loop Feedback Control	Accuracy of the Three-Dimensional Monitoring System
Li et al. [113]	2018	Laser confocal displacement meter	Yes	None (defects identified by visualization)	No	No	Not measured
Li et al. [114]	2021	Laser scanner	Yes	Geometric deviations from the CAD model	Yes	No	Mean and standard deviation of 3D deviation are 0 mm and 0.02 mm, respectively
Armstrong et al. [117]	2019	Laser scanner	Yes	Layer height and height difference from the CAD model	Yes	Yes	Not measured
Wi et al. [120]	2020	Structured light	No	Surface roughness	No	No	100 μm
Liu et al. [121]	2022	Structured light	Yes	Strain and stiffness	Yes	No	50 μm
Girard and Zhang [122]	2025	Structured light	Yes	Forced geometric error profile	Yes	Yes	Not measured
Holzmond and Li [123]	2017	3D DIC	Yes	Height difference from the CAD model	Yes	No	Not measured

Holzmond and Li [123] developed a topography monitoring method for the fused filament fabrication process using 3D digital image correlation (DIC). The 3D DIC system consisted of two cameras. The DIC method requires speckle patterns to establish a correlation between images taken at different time intervals [124,125]. However, the speckle patterns can be used to establish a correlation between the two camera images to estimate the depth. The authors used the grain pattern (natural texture) of the print sample (ColorFabb Woodfill Fine Filament) as the speckle patterns. Scanning was performed after each layer of printing, and the 3D topography was compared with the point cloud of the design model after registering the two point clouds to a global coordinate system. The depth difference was estimated from the two point clouds. Two types of defects were identified: (i) defects such as blobs/holes that cause a large local maxima/minima in the depth difference, and (ii) defects caused by extreme extrusion rates resulting in low/high average depth. However, the method was not robust as there were many factors, such as lighting conditions, grain pattern, etc., affecting the accuracy of the topography estimated

by the 3D DIC method. The method depends on the natural texture of the sample, which limits the use case of samples with uniform texture. Moreover, in order to accommodate the difference in density of the two point clouds, the authors transformed the point cloud data from the 3D DIC method, which smoothened many features in the point cloud.

5.3.2. Current State of Closed-Loop Feedback Control for Material Extrusion Based on In Situ 3D Surface Monitoring

Researchers have been able to achieve layer-wise closed-loop control in this field. Faes et al. [126] integrated a laser triangulation scanner to monitor the material extrusion process by detecting defects after each layer of printing. Armstrong et al. [117] created a laser scanner-based closed-loop monitoring system for extrusion bioprinting, which iteratively measured surface topography after each printed layer and compared it to the design model to calculate and correct printing errors through trajectory modifications.

There has also been research into incorporating real-time closed-loop control into this process. Kucukdeger et al. [127] developed a novel closed-loop controlled path-planning methodology for conformal 3D printing on moving substrates using real-time sensing of local object-tool offset that eliminated the need for global geometry descriptions. The system employed a 1D laser displacement sensor to provide feedback control of the microextrusion nozzle z-axis position, enabling printing on substrates oscillating at frequencies associated with human physiological processes (0.2–1.3 Hz).

Despite recent advances in process monitoring, implementing a fully autonomous closed-loop control system that can control and modify multiple input parameters and course-correct in real time for any in situ defects to minimize its impact on the final target part properties remains a significant challenge. This can be attributed to the fact that the interaction between the various process variables, like nozzle temperature and diameter, material viscosity, and feed rate, in conjunction with the environmental properties, can be quite complex and significantly impacts the final part quality. This makes it complex to establish a correlation between an in situ defect and the appropriate corrective action to minimize the defect in the final product. While emerging technologies in computer vision and machine learning show promise, the realization of fully autonomous process control systems that can ensure consistent product quality through immediate defect detection and correction requires further technological advancement.

5.4. In Situ 3D Monitoring for Material Jetting Processes: Current Practices and the State of Closed-Loop Feedback Control

Material jetting technology, characterized by its precise deposition of photopolymer droplets, offers exceptional surface finish and multi-material capabilities yet demands sophisticated monitoring solutions to maintain its high-precision requirements. Current in situ monitoring practices for these processes encompass advanced optical systems, droplet visualization techniques, and thermal imaging methods that collectively enable the real-time assessment of droplet formation, placement accuracy, and curing behavior.

5.4.1. Current Practices: 3D Surface Monitoring for Material Jetting

Sitthi-Amorn et al. [128] developed an OCT tool for monitoring the ink-jet printing process. The process monitoring framework involved the following steps: (i) a mask was generated based on the region where the material has to be printed, (ii) after printing a layer, the OCT system computed the depth within the masked region, and (iii) based on the height variation within the region an additional correction layer of printing was performed. In the correction layer, material printing was carried out only for the points that had a depth value below the average height of the sample. Although the method has a

closed-loop system for correcting printing errors, it will be difficult to perform real-time quality monitoring because of the time taken to complete an OCT scan.

Wang et al. [129] devised a liquid metal jet printing process setup with a vision-based monitoring system and closed-loop feedback control. They captured images of the piezoelectrically ejected droplets at a frequency of 300 Hz, used image processing techniques and analysis to calculate important parameters such as the number of satellites, size of ligament, jetting speed, and volume, and then mapped each set of properties to a voltage level. They trained a machine-learning model to be able to predict the voltage level of the jetter, given these properties as input, and used a PID controller to modify the voltage to achieve the target properties. The authors in this study were able to achieve real-time closed-loop feedback control with only 2D imaging. Three-dimensional imaging techniques such as structured light-based vision systems, which can image objects at Kilohertz speeds, could be easily incorporated into setups like these and can assist with directly capturing and measuring these parameters and perhaps even improve the accuracy of the measurements. This would lead to better quality data being fed to the machine-learning model and a better prediction accuracy for the voltage level.

5.4.2. Current State of Closed-Loop Feedback Control Based on In Situ 3D Surface Monitoring for Material Jetting

Real-time closed-loop feedback control has been achieved by researchers and commercial systems alike for this process. As mentioned previously, Wang et al. [129] deployed a real-time vision-based closed-loop control system which controlled voltage levels based on captured droplet images. Three-dimensional monitoring technology could be easily incorporated into setups like this to improve the accuracy of the measured geometric parameters and even capture additional data.

Commercial material jetting printers have also incorporated 3D vision-based monitoring and have been able to achieve closed-loop feedback control for this manufacturing process. Inkbit is a commercial device that employs a 3D vision system to achieve closed-loop feedback control to manufacture parts accurately at a production scale [130].

However, while real-time vision-based closed-loop feedback control has been achieved for this process both in research and commercially, a closed-loop control model that can continuously correct for defects that occur in situ in real time so that the final product created is still defect-free has not been established. This limitation stems from three key challenges: the high-speed dynamic nature of the process, the stochastic behavior of defect formation, and the complex relationship between in situ defect detection and appropriate real-time corrective actions. The high frequency of ejected droplets, the presence of multiple satellite droplets, the rapid shape change in droplets as they travel, and the interaction between the droplet and the powder bed are all dynamic factors that influence the final material properties. To achieve fully autonomous closed-loop control, it is important to model the impact of temperature (build chamber temperature, UV curing temperature, etc.), printhead (printhead speed, jetting frequency, drop deposition pattern, etc.), material (material viscosity, UV curing characteristics, etc.), and build (UV light intensity, build platform movement speed, etc.) parameters on these factors. This can be facilitated, in part, by real-time data collected by high-speed 3D monitoring and other sensing methods in conjunction with artificial intelligence. Machine learning could be used to develop predictive models that can anticipate potential defects and enable dynamic parameter adjustments, though significant research is still needed to achieve fully autonomous defect correction.

We have summarized representative studies that utilize in situ 3D monitoring technology for each AM process in Table 5.

Table 5. Representative literature on the use of 3D monitoring in various AM technologies.

Three-Dimensional Monitoring / AM Technologies	Digital Image Correlation	Laser Scanning	Structured Light	Optical Coherence Tomography
Powder Bed Fusion	N/A	Williams et al. [76].	Dickins et al. [66], Southon et al. [79], Zhang et al. [80], Zhang et al. [81], Land et al. [82], Liu et al. [83], Zhang et al. [84], Kalms et al. [85], Li et al. [86], Remani et al. [87], Liu et al. [88],	Kanko et al. [89], DePond et al. [90], Guan et al. [91], Lewis et al. [92], Gardner et al. [77]
Direct Energy Deposition	N/A	Heralic et al. [106], Tang et al. [108], Binega et al. [109]	Zhang et al. [110]	N/A
Material Extrusion	Holzmond and Li [123]	Li et al. [113], Armstrong et al. [117]	Wi et al. [120], Liu et al. [121], Girard and Zhang [122]	N/A
Material Jetting	N/A	N/A	N/A	Sitthi-Amorn et al. [128]

6. Discussion

Imaging systems have demonstrated the potential for improving the accuracy of AM parts through in situ monitoring. From the various research works discussed in Section 5, there are three prominent imaging techniques for monitoring AM processes: laser scanning, structured light systems, and optical coherence tomography. Laser scanning is a well-commercialized imaging method that can be integrated into any AM machine with ease. However, the limitation associated with laser scanning is that the scanning is carried out by projecting a laser line, and the laser line has to move across the entire surface of the object. Moreover, the accuracy of laser scanning is traded with the field of view, i.e., a laser scanner with high accuracy will have a small field of view [131]. On the other hand, a structured light system scans the entire surface by projecting fringe patterns. The surface topography can be estimated by projecting a minimum of three fringe patterns [64]. The compatibility of the structured light systems for monitoring powder bed fusion, DED, and material extrusion process has been demonstrated [83,85,110,121]. The accuracy of the system can be at the sub-micrometer level [132]. However, the system might have difficulties in imaging highly reflective metal objects because of the saturation caused by projector illumination. This problem has been widely analyzed by many researchers. For instance, Suresh et al. [95] proposed a high dynamic range-based imaging solution for saturated objects which works on the principle of utilizing the projector's bright and dark cycle. It involves capturing two images using the camera per projection cycle, performing phase shifting on the resulting sets of fringe pattern images, and fusing the resulting reconstructed depth maps. Zheng et al. [133] extended this to RGB cameras, where they captured images using an RGB camera and exploited the intensity response of red, green, and blue channels to obtain three different grayscale fringe images. Using image sets from each channel of the RGB image, they performed phase shifting on each of these, exploiting the varying degrees of intensity response of each of these channels (essentially equivalent to three sets of grayscale fringe pattern images at different levels of exposure), and fused the resulting reconstructed depth maps together to create a reconstruction without artifacts. Rao and Da [134] proposed a solution where they imaged a highly reflective object at multiple exposures and fused the resulting reconstructions together to remove artifacts. Though many research works have addressed this problem, there is no single method to completely suppress saturation-induced errors for all the objects.

The optical coherence tomography method does not suffer from this limitation. Among the three methods, OCT has the highest accuracy, which is under 1 µm [135]. However, the disadvantage is the time consumed for scanning. Additionally, the efficacy of OCT is dependent on process parameters such as laser power, scan speed, material properties, and the cooling rate. Excessive melt pool brightness can lead to oversaturation and poor data quality. There is also the interplay between the OCT scan speed and interlayer cooling rate. A fast scan speed can reduce the total build time but shorten interlayer cooling periods, which can lead to warping and porosity and impact microstructure homogeneity. Slower OCT scanning can extend interlayer cooling intervals but can increase overall build time and thereby decrease throughput [136]. OCT also generates large datasets and requires significant computational resources for real-time analysis. Multi-material components are difficult to reconstruct accurately due to their differing light absorption and reflection properties [137].

A summary of the three prominent 3D monitoring techniques for monitoring AM processes is listed in Table 6. However, while these techniques are the ones that are used most extensively in the literature, 3D monitoring techniques are not limited to the three technologies here.

The existing imaging methods have analyzed the surface topographies of AM parts for various defects such as surface roughness, irregularities, holes, melt pool depth, etc. Closed-loop feedback control is necessary to rectify the defects in the successive layers of printing. Few studies have implemented closed-loop feedback by altering the feed rate and other printing parameters to compensate for defects [106,108,110,117]. However, with the advancements in the machine learning field and the ability to provide real-time feedback, the application of machine-learning methods in the AM process has huge potential in realizing advanced feedback control. Using advanced 3D point cloud data processing networks such as PointNet [138] and PointNet++ [139], the 3D topography obtained from the imaging systems can be analyzed for precisely locating defects. This can be used to change the printing parameters in successive layers.

Table 6. Comprehensive summary of the three prominent 3D monitoring techniques for monitoring AM processes.

Three-Dimensional Monitoring Technology	Strengths of Monitoring Technology	Limitations of Monitoring Technology	AM Processes That the Technology Has Been Used to Monitor by Researchers
Laser Scanning	Well commercialized leading to easy integration with AM processes	Involves line-by-line scanning, leading to slower scan speeds; there exists an accuracy trade-off with field of view	Laser bed powder fusion, direct energy deposition, material extrusion, and material jetting
Structured Light	Superfast (up to kilohertz), can achieve sub-millimeter accuracy, and can perform simultaneous whole-area scanning	Occlusion/shadow regions and reflective surfaces	Laser bed powder fusion, direct energy deposition, and material extrusion
Optical Coherence Tomography	Has highest accuracy (under 1 µm)	Slowest scanning speed, making real-time process monitoring extremely challenging	Laser bed powder fusion, direct energy deposition, material extrusion, and material jetting

Additionally, current research explores the feedback control of a few parameters of these AM processes (e.g., laser power in LPBF and DED processes). However, high-speed,

real-time 3D monitoring techniques have the potential to capture copious amounts of data, including the 3D profile of the part, the shape of the melt pool in case of processes like LPBF and DED, the size and shape of droplets in case of processes like binder jetting and material jetting, which can then be used in conjunction with machine learning and reinforcement learning approaches to control a broad number of input parameters, perform real-time automated defect detection, and implement real-time corrective actions to mitigate/minimize defects in the final product. This can lead to a fully automated process and minimize defects and operational labor costs associated with these processes.

7. Summary

This paper summarized the existing research works on in situ 3D monitoring for additive manufacturing processes. The working principle of the different AM methods and 3D imaging methods have been explained. Various in situ 3D topography monitoring methods have been discussed for the four AM methods: (i) powder bed fusion, (ii) direct energy deposition, (iii) material extrusion, and (iv) material jetting. The inherent limitations in AM processes were described, and the potential combination of the surface monitoring methods to overcome the limitations was proposed. Additionally, we explored the current status and future outlook of closed-loop feedback control for these processes and discussed the ways in which 3D monitoring can bring us closer to fully automated additive manufacturing.

Author Contributions: Writing—original draft preparation, V.S., B.B., L.-H.Y. and B.L.; writing—review and editing, V.S., B.B. and B.L.; supervision, B.L.; project administration, B.L. All authors have read and agreed to the published version of the manuscript.

Funding: This work was funded in part by the REMADE Institute with award number 21-01-RM-5062.

Institutional Review Board Statement: Not applicable.

Informed Consent Statement: Not applicable.

Data Availability Statement: No new data were created or analyzed in this study. Data sharing is not applicable.

Acknowledgments: The authors would like to express gratitude to the REMADE Institute for their financial support. The views expressed here are those of the authors and are not necessarily those of the REMADE Institute.

Conflicts of Interest: The authors declare no conflicts of interest. The funders had no role in the design of the study; in the collection, analyses, or interpretation of data; in the writing of the manuscript; or in the decision to publish the results.

References

1. Akbari, M.; Ha, N. Impact of additive manufacturing on the Vietnamese transportation industry: An exploratory study. *Asian J. Shipp. Logist.* **2020**, *36*, 78–88. [CrossRef]
2. Khajavi, S.H. Additive manufacturing in the clothing industry: Towards sustainable new business models. *Appl. Sci.* **2021**, *11*, 8994. [CrossRef]
3. Hohn, M.M.; Durach, C.F. Additive manufacturing in the apparel supply chain—Impact on supply chain governance and social sustainability. *Int. J. Oper. Prod. Manag.* **2021**, *41*, 1035–1059. [CrossRef]
4. Özceylan, E.; Çetinkaya, C.; Demirel, N.; Sabırlıoğlu, O. Impacts of additive manufacturing on supply chain flow: A simulation approach in healthcare industry. *Logistics* **2017**, *2*, 1. [CrossRef]
5. Pinna, C.; Ramundo, L.; Sisca, F.G.; Angioletti, C.; Taisch, M.; Terzi, S. Additive Manufacturing applications within Food industry: An actual overview and future opportunities. In Proceedings of the Summer School Francesco Turco, Naples, Italy, 13–15 September 2016; pp. 18–24.
6. Mandache, C. Overview of non-destructive evaluation techniques for metal-based additive manufacturing. *Mater. Sci. Technol.* **2019**, *35*, 1007–1015. [CrossRef]

7. Li, N.; Link, G.; Engler, M.; Jelonnek, J. Small-size coaxial resonant applicator for microwave heating assisted additive manufacturing. *IEEE Trans. Microw. Theory Tech.* **2021**, *69*, 4631–4638. [CrossRef]
8. Ehlers, H.; Pelkner, M.; Thewes, R. Heterodyne eddy current testing using magnetoresistive sensors for additive manufacturing purposes. *IEEE Sensors J.* **2020**, *20*, 5793–5800. [CrossRef]
9. Dwivedi, S.K.; Vishwakarma, M.; Soni, A. Advances and researches on non destructive testing: A review. *Mater. Today Proc.* **2018**, *5*, 3690–3698. [CrossRef]
10. Buzug, T.M. Computed tomography. In *Springer Handbook of Medical Technology*; Springer: Berlin/Heidelberg, Germany, 2011; pp. 311–342.
11. Ritman, E.L. Micro-computed tomography—Current status and developments. *Annu. Rev. Biomed. Eng.* **2004**, *6*, 185–208. [CrossRef]
12. Raplee, J.; Plotkowski, A.; Kirka, M.M.; Dinwiddie, R.; Okello, A.; Dehoff, R.R.; Babu, S.S. Thermographic microstructure monitoring in electron beam additive manufacturing. *Sci. Rep.* **2017**, *7*, 43554. [CrossRef]
13. Thomas, T. Roughness and function. *Surf. Topogr. Metrol. Prop.* **2013**, *2*, 014001. [CrossRef]
14. Newton, L.; Senin, N.; Gomez, C.; Danzl, R.; Helmli, F.; Blunt, L.; Leach, R. Areal topography measurement of metal additive surfaces using focus variation microscopy. *Addit. Manuf.* **2019**, *25*, 365–389. [CrossRef]
15. Cai, Y.; Xiong, J.; Chen, H.; Zhang, G. A review of in-situ monitoring and process control system in metal-based laser additive manufacturing. *J. Manuf. Syst.* **2023**, *70*, 309–326. [CrossRef]
16. Özel, T. A review on in-situ process sensing and monitoring systems for fusion-based additive manufacturing. *Int. J. Mechatron. Manuf. Syst.* **2023**, *16*, 115–154. [CrossRef]
17. Aydogan, B.; Chou, K. Review of In Situ Detection and Ex Situ Characterization of Porosity in Laser Powder Bed Fusion Metal Additive Manufacturing. *Metals* **2024**, *14*, 669. [CrossRef]
18. Balhara, H.; Karthikeyan, A.; Hanchate, A.; Nakkina, T.G.; Bukkapatnam, S.T.S. Imaging systems and techniques for fusion-based metal additive manufacturing: A review. *Front. Manuf. Technol.* **2023**, *3*, 1271190. [CrossRef]
19. Chen, L.; Bi, G.; Yao, X.; Su, J.; Tan, C.; Feng, W.; Benakis, M.; Chew, Y.; Moon, S.K. In-situ process monitoring and adaptive quality enhancement in laser additive manufacturing: A critical review. *J. Manuf. Syst.* **2024**, *74*, 527–574. [CrossRef]
20. AbouelNour, Y.; Gupta, N. In-situ monitoring of sub-surface and internal defects in additive manufacturing: A review. *Mater. Des.* **2022**, *222*, 111063. [CrossRef]
21. Zhang, Y.; Shen, S.; Li, H.; Hu, Y. Review of in situ and real-time monitoring of metal additive manufacturing based on image processing. *Int. J. Adv. Manuf. Technol.* **2022**, *123*, 1–20. [CrossRef]
22. Xia, C.; Pan, Z.; Polden, J.; Li, H.; Xu, Y.; Chen, S.; Zhang, Y. A review on wire arc additive manufacturing: Monitoring, control and a framework of automated system. *J. Manuf. Syst.* **2020**, *57*, 31–45. [CrossRef]
23. Lu, Q.Y.; Wong, C.H. Additive manufacturing process monitoring and control by non-destructive testing techniques: Challenges and in-process monitoring. *Virtual Phys. Prototyp.* **2018**, *13*, 39–48. [CrossRef]
24. Everton, S.K.; Hirsch, M.; Stravroulakis, P.; Leach, R.K.; Clare, A.T. Review of in-situ process monitoring and in-situ metrology for metal additive manufacturing. *Mater. Des.* **2016**, *95*, 431–445. [CrossRef]
25. Oleff, A.; Küster, B.; Stonis, M.; Overmeyer, L. Process monitoring for material extrusion additive manufacturing: A state-of-the-art review. *Prog. Addit. Manuf.* **2021**, *6*, 705–730. [CrossRef]
26. Jacob, J.; Pejak Simunec, D.; Kandjani, A.E.; Trinchi, A.; Sola, A. A Review of Fused Filament Fabrication of Metal Parts (Metal FFF): Current Developments and Future Challenges. *Technologies* **2024**, *12*, 267. [CrossRef]
27. Vora, H.D.; Sanyal, S. A comprehensive review: Metrology in additive manufacturing and 3D printing technology. *Prog. Addit. Manuf.* **2020**, *5*, 319–353. [CrossRef]
28. Sun, S.; Brandt, M.; Easton, M. Powder bed fusion processes: An overview. *Laser Addit. Manuf.* **2017**, 55–77. [CrossRef]
29. Singh, D.D.; Mahender, T.; Reddy, A.R. Powder bed fusion process: A brief review. *Mater. Today Proc.* **2021**, *46*, 350–355. [CrossRef]
30. Tang, M.; Pistorius, P.C.; Beuth, J.L. Prediction of lack-of-fusion porosity for powder bed fusion. *Addit. Manuf.* **2017**, *14*, 39–48. [CrossRef]
31. Hou, Z.J.; Wang, Q.; Zhao, C.G.; Zheng, J.; Tian, J.M.; Ge, X.H.; Liu, Y.G. Online Monitoring Technology of Metal Powder Bed Fusion Processes: A Review. *Materials* **2022**, *15*, 7598. [CrossRef]
32. Gibson, I.; Rosen, D.; Stucker, B.; Gibson, I.; Rosen, D.; Stucker, B. Directed energy deposition processes. In *Additive Manufacturing Technologies: 3D Printing, Rapid Prototyping, and Direct Digital Manufacturing*; Springer: New York, NY, USA, 2015; pp. 245–268.
33. Ahn, D.G. Directed energy deposition (DED) process: State of the art. *Int. J. Precis. Eng. Manuf.-Green Technol.* **2021**, *8*, 703–742. [CrossRef]
34. Dávila, J.L.; Neto, P.I.; Noritomi, P.Y.; Coelho, R.T.; da Silva, J.V.L. Hybrid manufacturing: A review of the synergy between directed energy deposition and subtractive processes. *Int. J. Adv. Manuf. Technol.* **2020**, *110*, 3377–3390. [CrossRef]

35. Tang, Z.J.; Liu, W.W.; Wang, Y.W.; Saleheen, K.M.; Liu, Z.C.; Peng, S.T.; Zhang, Z.; Zhang, H.C. A review on in situ monitoring technology for directed energy deposition of metals. *Int. J. Adv. Manuf. Technol.* **2020**, *108*, 3437–3463. [CrossRef]
36. Goh, G.D.; Yap, Y.L.; Tan, H.; Sing, S.L.; Goh, G.L.; Yeong, W.Y. Process–structure–properties in polymer additive manufacturing via material extrusion: A review. *Crit. Rev. Solid State Mater. Sci.* **2020**, *45*, 113–133. [CrossRef]
37. Hsiang Loh, G.; Pei, E.; Gonzalez-Gutierrez, J.; Monzón, M. An overview of material extrusion troubleshooting. *Appl. Sci.* **2020**, *10*, 4776. [CrossRef]
38. Gülcan, O.; Günaydın, K.; Tamer, A. The state of the art of material jetting—A critical review. *Polymers* **2021**, *13*, 2829. [CrossRef] [PubMed]
39. Gibson, I.; Rosen, D.; Stucker, B.; Khorasani, M.; Gibson, I.; Rosen, D.; Stucker, B.; Khorasani, M. Material jetting. In *Additive Manufacturing Technologies*; Springer: Boston, MA, USA, 2021; pp. 203–235.
40. Ogunsanya, M.; Isichei, J.; Parupelli, S.K.; Desai, S.; Cai, Y. In-Situ Droplet Monitoring Inkjet 3D Printing Process Using Image Analysis Machine Learning Models. *Procedia Manuf.* **2021**, *53*, 427–434. [CrossRef]
41. Cunha, F.G.; Santos, T.G.; Xavier, J. In Situ Monitoring of Additive Manufacturing Using Digital Image Correlation: A Review. *Materials* **2021**, *14*, 1511. [CrossRef]
42. Gibson, I.; Rosen, D.; Stucker, B.; Gibson, I.; Rosen, D.; Stucker, B. Vat photopolymerization processes. In *Additive Manufacturing Technologies: 3D Printing, Rapid Prototyping, and Direct Digital Manufacturing*; Springer: New York, NY, USA, 2015; pp. 63–106.
43. Yang, F.; Kazi, A.; Marmo, A.; Grunlan, M.A.; Tai, B.L. Characterizing the separation behavior of photocurable PDMS on a hydrogel film during vat photopolymerization: A benchmark study. *Addit. Manuf.* **2022**, *58*, 103070. [CrossRef]
44. Paral, S.K.; Lin, D.Z.; Cheng, Y.L.; Lin, S.C.; Jeng, J.Y. A Review of Critical Issues in High-Speed Vat Photopolymerization. *Polymers* **2023**, *15*, 2716. [CrossRef]
45. Gibson, I.; Rosen, D.; Stucker, B.; Khorasani, M.; Gibson, I.; Rosen, D.; Stucker, B.; Khorasani, M. Binder jetting. In *Additive Manufacturing Technologies*; Springer: Boston, MA, USA, 2021; pp. 237–252.
46. Mostafaei, A.; Elliott, A.M.; Barnes, J.E.; Li, F.; Tan, W.; Cramer, C.L.; Nandwana, P.; Chmielus, M. Binder jet 3D printing—Process parameters, materials, properties, modeling, and challenges. *Prog. Mater. Sci.* **2021**, *119*, 100707. [CrossRef]
47. Konda Gokuldoss, P.; Kolla, S.; Eckert, J. Additive manufacturing processes: Selective laser melting, electron beam melting and binder jetting—Selection guidelines. *Materials* **2017**, *10*, 672. [CrossRef] [PubMed]
48. Parab, N.D.; Barnes, J.E.; Zhao, C.; Cunningham, R.W.; Fezzaa, K.; Rollett, A.D.; Sun, T. Real time observation of binder jetting printing process using high-speed X-ray imaging. *Sci. Rep.* **2019**, *9*, 2499. [CrossRef]
49. Gibson, I.; Rosen, D.W.; Stucker, B.; Gibson, I.; Rosen, D.W.; Stucker, B. Sheet lamination processes. In *Additive Manufacturing Technologies: Rapid Prototyping to Direct Digital Manufacturing*; Springer: Boston, MA, USA, 2010; pp. 223–252.
50. Gibson, I.; Rosen, D.; Stucker, B.; Khorasani, M.; Gibson, I.; Rosen, D.; Stucker, B.; Khorasani, M. Sheet lamination. In *Additive Manufacturing Technologies*; Springer: Boston, MA, USA, 2021; pp. 253–283.
51. Hu, Z.; Xie, H.; Lu, J.; Hua, T.; Zhu, J. Study of the performance of different subpixel image correlation methods in 3D digital image correlation. *Appl. Opt.* **2010**, *49*, 4044–4051. [CrossRef] [PubMed]
52. Sutton, M.A.; Yan, J.; Tiwari, V.; Schreier, H.; Orteu, J.J. The effect of out-of-plane motion on 2D and 3D digital image correlation measurements. *Opt. Lasers Eng.* **2008**, *46*, 746–757. [CrossRef]
53. Helfrick, M.N.; Niezrecki, C.; Avitabile, P.; Schmidt, T. 3D digital image correlation methods for full-field vibration measurement. *Mech. Syst. Signal Process.* **2011**, *25*, 917–927. [CrossRef]
54. Gu, G. A comparative study of random speckle pattern simulation models in digital image correlation. *Optik* **2015**, *126*, 3713–3716. [CrossRef]
55. Axelsson, P. Processing of laser scanner data—Algorithms and applications. *ISPRS J. Photogramm. Remote Sens.* **1999**, *54*, 138–147. [CrossRef]
56. França, J.G.D.; Gazziro, M.A.; Ide, A.N.; Saito, J.H. A 3D scanning system based on laser triangulation and variable field of view. In Proceedings of the IEEE International Conference on Image Processing 2005, Genova, Italy, 14 September 2005; Volume 1, pp. 1–425.
57. Acosta, D.; García, O.; Aponte, J. Laser triangulation for shape acquisition in a 3D scanner plus scan. In Proceedings of the Electronics, Robotics and Automotive Mechanics Conference (CERMA'06), Cuernavaca, Mexico, 26–29 September 2006; Volume 2, pp. 14–19.
58. Payeur, P.; Desjardins, D. Structured light stereoscopic imaging with dynamic pseudo-random patterns. In Proceedings of the Image Analysis and Recognition: 6th International Conference, ICIAR 2009, Halifax, NS, Canada, 6–8 July 2009; Proceedings 6; Springer: Berlin/Heidelberg, Germany, 2009; pp. 687–696.
59. Salvi, J.; Pages, J.; Batlle, J. Pattern codification strategies in structured light systems. *Pattern Recognit.* **2004**, *37*, 827–849. [CrossRef]
60. Carrihill, B.; Hummel, R. Experiments with the intensity ratio depth sensor. *Comput. Vision Graph. Image Process.* **1985**, *32*, 337–358. [CrossRef]

61. Huang, P.S.; Zhang, S. Fast three-step phase-shifting algorithm. *Appl. Opt.* **2006**, *45*, 5086–5091. [CrossRef]
62. Zhang, S.; Huang, P.S. Novel method for structured light system calibration. *Opt. Eng.* **2006**, *45*, 083601.
63. Li, B.; Karpinsky, N.; Zhang, S. Novel calibration method for structured-light system with an out-of-focus projector. *Appl. Opt.* **2014**, *53*, 3415–3426. [CrossRef]
64. Zhang, S. Recent progresses on real-time 3D shape measurement using digital fringe projection techniques. *Opt. Lasers Eng.* **2010**, *48*, 149–158. [CrossRef]
65. Lu, L.; Suresh, V.; Zheng, Y.; Wang, Y.; Xi, J.; Li, B. Motion induced error reduction methods for phase shifting profilometry: A review. *Opt. Lasers Eng.* **2021**, *141*, 106573. [CrossRef]
66. Dickins, A.; Widjanarko, T.; Sims-Waterhouse, D.; Thompson, A.; Lawes, S.; Senin, N.; Leach, R. Multi-view fringe projection system for surface topography measurement during metal powder bed fusion. *J. Opt. Soc. Am. A* **2020**, *37*, B93. [CrossRef] [PubMed]
67. Rebolleda, G.; Diez-Alvarez, L.; Casado, A.; Sánchez-Sánchez, C.; De Dompablo, E.; González-López, J.J.; Muñoz-Negrete, F.J. OCT: New perspectives in neuro-ophthalmology. *Saudi J. Ophthalmol.* **2015**, *29*, 9–25. [CrossRef]
68. Schmitt, J.M. Optical coherence tomography (OCT): A review. *IEEE J. Sel. Top. Quantum Electron.* **1999**, *5*, 1205–1215. [CrossRef]
69. Podoleanu, A.G.; Rogers, J.A.; Jackson, D.A.; Dunne, S. Three dimensional OCT images from retina and skin. *Opt. Express* **2000**, *7*, 292–298. [CrossRef]
70. Fujimoto, J.G.; Drexler, W.; Schuman, J.S.; Hitzenberger, C.K. Optical Coherence Tomography (OCT) in ophthalmology: Introduction. *Opt. Express* **2009**, *17*, 3978–3979. [CrossRef]
71. Fujimoto, J.; Swanson, E. The development, commercialization, and impact of optical coherence tomography. *Investig. Ophthalmol. Vis. Sci.* **2016**, *57*, OCT1–OCT13. [CrossRef]
72. Podoleanu, A.G. Optical coherence tomography. *J. Microsc.* **2012**, *247*, 209–219. [CrossRef] [PubMed]
73. Zorin, I.; Brouczek, D.; Geier, S.; Nohut, S.; Eichelseder, J.; Huss, G.; Schwentenwein, M.; Heise, B. Mid-infrared optical coherence tomography as a method for inspection and quality assurance in ceramics additive manufacturing. *Open Ceram.* **2022**, *12*, 100311. [CrossRef]
74. Bartlett, J.L.; Jarama, A.; Jones, J.; Li, X. Prediction of microstructural defects in additive manufacturing from powder bed quality using digital image correlation. *Mater. Sci. Eng. A* **2020**, *794*, 140002. [CrossRef]
75. Ma, D.; Tian, X.; Chang, T.; Hussain, S.; Xia, L.; Han, J. In-Situ Process Monitoring and Optimization for Extrusion-Based Silicone Additive Manufacturing. In *International Manufacturing Science and Engineering Conference*; American Society of Mechanical Engineers: New York, NY, USA, 2024. [CrossRef]
76. Williams, R.J.; Davies, C.M.; Hooper, P.A. In situ monitoring of the layer height in laser powder bed fusion. *Mater. Des. Process. Commun.* **2021**, *3*, e173. [CrossRef]
77. Gardner, M.R.; Lewis, A.; Park, J.; McElroy, A.B.; Estrada, A.D.; Fish, S.; Beaman, J.J.; Milner, T.E. In situ process monitoring in selective laser sintering using optical coherence tomography. *Opt. Eng.* **2018**, *57*, 041407. [CrossRef]
78. Foster, B.; Reutzel, E.; Nassar, A.; Hall, B.; Brown, S.; Dickman, C. Optical, layerwise monitoring of powder bed fusion. In Proceedings of the 2014 International Solid Freeform Fabrication Symposium, Austin, TX, USA, 4–6 August 2014.
79. Southon, N.; Stavroulakis, P.; Goodridge, R.; Leach, R. In-process measurement and monitoring of a polymer laser sintering powder bed with fringe projection. *Mater. Des.* **2018**, *157*, 227–234. [CrossRef]
80. Zhang, H.; Vallabh, C.K.P.; Xiong, Y.; Zhao, X. A systematic study and framework of fringe projection profilometry with improved measurement performance for in-situ LPBF process monitoring. *Measurement* **2022**, *191*, 110796. [CrossRef]
81. Zhang, H.; Vallabh, C.K.P.; Zhao, X. Machine learning enhanced high dynamic range fringe projection profilometry for in-situ layer-wise surface topography measurement during LPBF additive manufacturing. *Precis. Eng.* **2023**, *84*, 1–14. [CrossRef]
82. Land II, W.S.; Zhang, B.; Ziegert, J.; Davies, A. In-situ metrology system for laser powder bed fusion additive process. *Procedia Manuf.* **2015**, *1*, 393–403. [CrossRef]
83. Liu, Y.; Blunt, L.; Zhang, Z.; Rahman, H.A.; Gao, F.; Jiang, X. In-situ areal inspection of powder bed for electron beam fusion system based on fringe projection profilometry. *Addit. Manuf.* **2020**, *31*, 100940. [CrossRef]
84. Zhang, B.; Ziegert, J.; Farahi, F.; Davies, A. In situ surface topography of laser powder bed fusion using fringe projection. *Addit. Manuf.* **2016**, *12*, 100–107. [CrossRef]
85. Kalms, M.; Narita, R.; Thomy, C.; Vollertsen, F.; Bergmann, R.B. New approach to evaluate 3D laser printed parts in powder bed fusion-based additive manufacturing in-line within closed space. *Addit. Manuf.* **2019**, *26*, 161–165. [CrossRef]
86. Li, Z.; Liu, X.; Wen, S.; He, P.; Zhong, K.; Wei, Q.; Shi, Y.; Liu, S. In situ 3D monitoring of geometric signatures in the powder-bed-fusion additive manufacturing process via vision sensing methods. *Sensors* **2018**, *18*, 1180. [CrossRef]
87. Remani, A.; Rossi, A.; Peña, F.; Thompson, A.; Dardis, J.; Jones, N.; Senin, N.; Leach, R. In-situ monitoring of laser-based powder bed fusion using fringe projection. *Addit. Manuf.* **2024**, *90*, 104334. [CrossRef]
88. Liu, Y.; Blunt, L.; Gao, F.; Jiang, X. High-dynamic-range 3D measurement for E-beam fusion additive manufacturing based on SVM intelligent fringe projection system. *Surf. Topogr. Metrol. Prop.* **2021**, *9*, 034002. [CrossRef]

89. Kanko, J.A.; Sibley, A.P.; Fraser, J.M. In situ morphology-based defect detection of selective laser melting through inline coherent imaging. *J. Mater. Process. Technol.* **2016**, *231*, 488–500. [CrossRef]
90. DePond, P.J.; Guss, G.; Ly, S.; Calta, N.P.; Deane, D.; Khairallah, S.; Matthews, M.J. In situ measurements of layer roughness during laser powder bed fusion additive manufacturing using low coherence scanning interferometry. *Mater. Des.* **2018**, *154*, 347–359. [CrossRef]
91. Guan, G.; Hirsch, M.; Lu, Z.H.; Childs, D.T.; Matcher, S.J.; Goodridge, R.; Groom, K.M.; Clare, A.T. Evaluation of selective laser sintering processes by optical coherence tomography. *Mater. Des.* **2015**, *88*, 837–846. [CrossRef]
92. Lewis, A.; Gardner, M.; McElroy, A.; Milner, T.; Fish, S.; Beaman, J. In-situ process monitoring and ex-situ part quality assessment of selective laser sintering using optical coherence tomography. In Proceedings of the 2016 International Solid Freeform Fabrication Symposium, Austin, TX, USA, 8–10 August 2016.
93. Eschner, E.; Staudt, T.; Schmidt, M. 3D particle tracking velocimetry for the determination of temporally resolved particle trajectories within laser powder bed fusion of metals. *Int. J. Extrem. Manuf.* **2019**, *1*, 035002. [CrossRef]
94. Welch, G.; Bishop, G. *An Introduction to the Kalman Filter*; University of North Carolina: Chapel Hill, NC, USA, 1995.
95. Suresh, V.; Wang, Y.; Li, B. High-dynamic-range 3D shape measurement utilizing the transitioning state of digital micromirror device. *Opt. Lasers Eng.* **2018**, *107*, 176–181. [CrossRef]
96. Dabov, K.; Foi, A.; Katkovnik, V.; Egiazarian, K. Image denoising with block-matching and 3D filtering. In Proceedings of the SPIE—The International Society for Optical Engineering, Image Processing: Algorithms and Systems, Neural Networks, and Machine Learning, San Jose, CA, USA, 25–26 January 2006; Volume 6064, pp. 354–365.
97. Wang, R.; Standfield, B.; Dou, C.; Law, A.C.; Kong, Z.J. Real-time process monitoring and closed-loop control on laser power via a customized laser powder bed fusion platform. *Addit. Manuf.* **2023**, *66*, 103449. [CrossRef]
98. Vasileska, E.; Demir, A.G.; Colosimo, B.M.; Previtali, B. Layer-wise control of selective laser melting by means of inline melt pool area measurements. *J. Laser Appl.* **2020**, *32*, 022057. [CrossRef]
99. Shkoruta, A.; Mishra, S.; Rock, S.J. Real-Time Image-Based Feedback Control of Laser Powder Bed Fusion. *ASME Lett. Dyn. Syst. Control* **2021**, *2*, 021001. [CrossRef]
100. Montazeri, M.; Yavari, R.; Rao, P.; Boulware, P. In-Process Monitoring of Material Cross-Contamination Defects in Laser Powder Bed Fusion. *J. Manuf. Sci. Eng.* **2018**, *140*, 111001. [CrossRef]
101. Guerra, M.G.; Errico, V.; Fusco, A.; Lavecchia, F.; Campanelli, S.L.; Galantucci, L.M. High resolution-optical tomography for in-process layerwise monitoring of a laser-powder bed fusion technology. *Addit. Manuf.* **2022**, *55*, 102850. [CrossRef]
102. Gaikwad, A.; Williams, R.J.; de Winton, H.; Bevans, B.D.; Smoqi, Z.; Rao, P.; Hooper, P.A. Multi phenomena melt pool sensor data fusion for enhanced process monitoring of laser powder bed fusion additive manufacturing. *Mater. Des.* **2022**, *221*, 110919. [CrossRef]
103. Zou, Z.; Zhang, K.; Liu, T.; Li, J.; Zhu, Z.; Wei, H.; Lu, Y.; Liao, W. In situ monitoring with melt pool data based on multi-signal fusion method in laser powder bed fusion. *Measurement* **2024**, *234*, 114877. [CrossRef]
104. Wang, P.; Yang, Y.; Moghaddam, N.S. Process modeling in laser powder bed fusion towards defect detection and quality control via machine learning: The state-of-the-art and research challenges. *J. Manuf. Process.* **2022**, *73*, 961–984. [CrossRef]
105. Liu, C.; Roux, L.L.; Ji, Z.; Kerfriden, P.; Lacan, F.; Bigot, S. Machine Learning-enabled feedback loops for metal powder bed fusion additive manufacturing. *Procedia Comput. Sci.* **2020**, *176*, 2586–2595. [CrossRef]
106. Heralić, A.; Christiansson, A.K.; Lennartson, B. Height control of laser metal-wire deposition based on iterative learning control and 3D scanning. *Opt. Lasers Eng.* **2012**, *50*, 1230–1241. [CrossRef]
107. Wallén, J. Estimation-Based Iterative Learning Control. Ph.D. Thesis, Linköping University, Linköping, Sweden, 2011.
108. Tang, S.; Wang, G.; Zhang, H. In situ 3D monitoring and control of geometric signatures in wire and arc additive manufacturing. *Surf. Topogr. Metrol. Prop.* **2019**, *7*, 025013. [CrossRef]
109. Binega, E.; Yang, L.; Sohn, H.; Cheng, J.C. Online geometry monitoring during directed energy deposition additive manufacturing using laser line scanning. *Precis. Eng.* **2022**, *73*, 104–114. [CrossRef]
110. Zhang, X.; Shen, W.; Suresh, V.; Hamilton, J.; Yeh, L.H.; Jiang, X.; Zhang, Z.; Li, Q.; Li, B.; Rivero, I.V.; et al. In situ monitoring of direct energy deposition via structured light system and its application in remanufacturing industry. *Int. J. Adv. Manuf. Technol.* **2021**, *116*, 959–974. [CrossRef]
111. Akbari, M.; Kovacevic, R. Closed loop control of melt pool width in robotized laser powder–directed energy deposition process. *Int. J. Adv. Manuf. Technol.* **2019**, *104*, 2887–2898. [CrossRef]
112. Gibson, B.T.; Bandari, Y.K.; Richardson, B.S.; Henry, W.C.; Vetland, E.J.; Sundermann, T.W.; Love, L.J. Melt pool size control through multiple closed-loop modalities in laser-wire directed energy deposition of Ti-6Al-4V. *Addit. Manuf.* **2020**, *32*, 100993. [CrossRef]
113. Li, L.; McGuan, R.; Kavehpour, P.; Candler, R. Precision enhancement of 3D printing via in situ metrology. In Proceedings of the 2018 International Solid Freeform Fabrication Symposium, Austin, TX, USA, 13–15 August 2018.

114. Li, L.; McGuan, R.; Isaac, R.; Kavehpour, P.; Candler, R. Improving precision of material extrusion 3D printing by in-situ monitoring & predicting 3D geometric deviation using conditional adversarial networks. *Addit. Manuf.* **2021**, *38*, 101695.
115. Besl, P.J.; McKay, N.D. Method for registration of 3-D shapes. In Proceedings of the Sensor Fusion IV: Control Paradigms and Data Structures, Boston, MA, USA, 12–15 November 1991; SPIE: Bellingham, DC, USA, 1992; Volume 1611, pp. 586–606.
116. Isola, P.; Zhu, J.Y.; Zhou, T.; Efros, A.A. Image-to-image translation with conditional adversarial networks. In Proceedings of the IEEE Conference on Computer Vision and Pattern Recognition, Honolulu, HI, USA, 21–26 July 2017; pp. 1125–1134.
117. Armstrong, A.A.; Norato, J.; Alleyne, A.G.; Johnson, A.J.W. Direct process feedback in extrusion-based 3D bioprinting. *Biofabrication* **2019**, *12*, 015017. [CrossRef]
118. Nuchitprasitchai, S. An Algorithm for Reconstructing Three-Dimensional Images from Overlapping Two-Dimensional Intensity Measurements with Relaxed Camera Positioning Requirements, with Application to Additive Manufacturing. Ph.D. Thesis, Michigan Technological University, Houghton, MI, USA, 2017; ISBN 9780355316131.
119. Nuchitprasitchai, S.; Roggemann, M.; Pearce, J.M. Factors effecting real-time optical monitoring of fused filament 3D printing. *Prog. Addit. Manuf.* **2017**, *2*, 133–149. [CrossRef]
120. Wi, K.; Suresh, V.; Wang, K.; Li, B.; Qin, H. Quantifying quality of 3D printed clay objects using a 3D structured light scanning system. *Addit. Manuf.* **2020**, *32*, 100987. [CrossRef]
121. Liu, X.; Kan, C.; Ye, Z. Real-time multiscale prediction of structural performance in material extrusion additive manufacturing. *Addit. Manuf.* **2022**, *49*, 102503. [CrossRef]
122. Girard, J.; Zhang, S. Fast error detection method for additive manufacturing process monitoring using structured light three dimensional imaging technique. *Opt. Lasers Eng.* **2025**, *184*, 108609. [CrossRef]
123. Holzmond, O.; Li, X. In situ real time defect detection of 3D printed parts. *Addit. Manuf.* **2017**, *17*, 135–142. [CrossRef]
124. Niblack, W. *An Introduction to Digital Image Processing*; Strandberg Publishing Company: Hovedstaden Denmark, 1985.
125. Pan, B.; Qian, K.; Xie, H.; Asundi, A. Two-dimensional digital image correlation for in-plane displacement and strain measurement: A review. *Meas. Sci. Technol.* **2009**, *20*, 062001. [CrossRef]
126. Faes, M.; Abbeloos, W.; Vogeler, F.; Valkenaers, H.; Coppens, K.; Goedemé, T.; Ferraris, E. Process Monitoring of Extrusion Based 3D Printing via Laser Scanning. *arXiv* **2014**, arXiv:1612.02219. [CrossRef]
127. Kucukdeger, E.; Johnson, B.N. Closed-loop controlled conformal 3D printing on moving objects via tool-localized object position sensing. *J. Manuf. Process.* **2023**, *89*, 39–49. [CrossRef]
128. Sitthi-Amorn, P.; Ramos, J.E.; Wangy, Y.; Kwan, J.; Lan, J.; Wang, W.; Matusik, W. MultiFab: A machine vision assisted platform for multi-material 3D printing. *Acm Trans. Graph. (Tog)* **2015**, *34*, 1–11. [CrossRef]
129. Wang, T.; Kwok, T.H.; Zhou, C.; Vader, S. *In-Situ* Droplet Inspection and Closed-Loop Control System Using Machine Learning for Liquid Metal Jet Printing. *J. Manuf. Syst.* **2018**, *47*, 83–92. [CrossRef]
130. Inkbit Technology: 3D Printing Enhanced by Vision-Controlled Jetting (VCJ). Available online: https://inkbit3d.com/technology/ (accessed on 17 April 2025).
131. Boehler, W.; Vicent, M.B.; Marbs, A. Investigating laser scanner accuracy. *Int. Arch. Photogramm. Remote Sens. Spat. Inf. Sci.* **2003**, *34*, 696–701.
132. Li, B.; Zhang, S. Flexible calibration method for microscopic structured light system using telecentric lens. *Opt. Express* **2015**, *23*, 25795–25803. [CrossRef]
133. Zheng, Y.; Wang, Y.; Suresh, V.; Li, B. Real-time high-dynamic-range fringe acquisition for 3D shape measurement with a RGB camera. *Meas. Sci. Technol.* **2019**, *30*, 075202. . [CrossRef]
134. Rao, L.; Da, F. High dynamic range 3D shape determination based on automatic exposure selection. *J. Vis. Commun. Image Represent.* **2018**, *50*, 217–226. [CrossRef]
135. Park, B.H.; Pierce, M.C.; Cense, B.; Yun, S.H.; Mujat, M.; Tearney, G.J.; Bouma, B.E.; de Boer, J.F. Real-time fiber-based multi-functional spectral-domain optical coherence tomography at 1.3 µm. *Opt. Express* **2005**, *13*, 3931–3944. [CrossRef] [PubMed]
136. Estalaki, S.M.; Lough, C.S.; Landers, R.G.; Kinzel, E.C.; Luo, T. Predicting defects in laser powder bed fusion using in-situ thermal imaging data and machine learning. *Addit. Manuf.* **2022**, *58*, 103008. [CrossRef]
137. Dharnidharka, M.; Chadha, U.; Dasari, L.M.; Paliwal, A.; Surya, Y.; Selvaraj, S.K. Optical tomography in additive manufacturing: A review, processes, open problems, and new opportunities. *Eur. Phys. J. Plus* **2021**, *136*, 1133. [CrossRef]
138. Qi, C.R.; Su, H.; Mo, K.; Guibas, L.J. Pointnet: Deep learning on point sets for 3d classification and segmentation. In Proceedings of the IEEE Conference on Computer Vision and Pattern Recognition, Honolulu, HI, USA, 21–26 July 2017; pp. 652–660.
139. Qi, C.R.; Yi, L.; Su, H.; Guibas, L.J. Pointnet++: Deep hierarchical feature learning on point sets in a metric space. *Adv. Neural Inf. Process. Syst.* **2017**, *30*, 5105–5114.

Disclaimer/Publisher's Note: The statements, opinions and data contained in all publications are solely those of the individual author(s) and contributor(s) and not of MDPI and/or the editor(s). MDPI and/or the editor(s) disclaim responsibility for any injury to people or property resulting from any ideas, methods, instructions or products referred to in the content.